ANCR-NUREG-1340
DATE PUBLISHED — SEPTEMBER 1976

IDAHO NATIONAL ENGINEERING LABORATORY

NUMERICAL METHODS FOR SOLVING THE GOVERNING EQUATIONS FOR A SERIATED CONTINUUM

ROBERT E. NARUM
CHARLES NOBLE
GLEN A. MORTENSEN
JAMES H. McFADDEN

PREPARED BY AEROJET NUCLEAR COMPANY FOR
U. S. NUCLEAR REGULATORY COMMISSION
AND
ENERGY RESEARCH AND DEVELOPMENT ADMINISTRATION
IDAHO OPERATIONS OFFICE UNDER CONTRACT E(10-1)-1375

DISCLAIMER

Printed in the United States of America
Available from
National Technical Information Service
U. S. Department of Commerce
5285 Port Royal Road
Springfield, Virginia 22161
Price: Printed Copy $4.00; Microfiche $2.25

"The NRC will make available data tapes and operational computer codes on research programs dealing with postulated loss-of-coolant accidents in light water reactors. Persons requesting this information must reimburse the NRC contractors for their expenses in preparing copies of the data tapes and the operational computer codes. Requests should be submitted to the Research Applications Branch, Office of Nuclear Regulatory Research, Nuclear Regulatory Commission, Washington, D.C. 20555."

ANCR-NUREG-1340

Distributed Under Category:
NRC-4
Water Reactor Safety Research
Analysis Development

NUMERICAL METHODS FOR SOLVING THE GOVERNING EQUATIONS FOR A SERIATED CONTINUUM

by

Robert E. Narum, Aerojet Nuclear Company
Charles Noble, Aerojet Nuclear Company
Glen A. Mortensen, Intermountain Technologies Incorporated
James H. McFadden, Energy Incorporated

AEROJET NUCLEAR COMPANY

Date Published – September 1976

PREPARED FOR THE
U.S. NUCLEAR REGULATORY COMMISSION
AND
ENERGY RESEARCH AND DEVELOPMENT ADMINISTRATION
IDAHO OPERATIONS OFFICE
UNDER CONTRACT NO. E (10-1)-1375

ACKNOWLEDGMENTS

The work reported in this document was a group effort sponsored by the Reactor Behavior Program. The following individuals contributed to the group effort:

E. D. Hughes

C. W. Solbrig

C. F. Obenchain

R. W. Lyczkowski

W. J. Suitt

J. A. Trapp

ABSTRACT

A desire to more accurately predict the behavior of transient two-phase flows has resulted in an investigation of the feasibility of computing unequal phase velocities and unequal phase temperatures. The finite difference forms of a set of equations governing a seriated continuum are presented along with two methods developed for solving the resulting systems of simultaneous nonlinear equations. Results from a one-dimensional computer code are presented to illustrate the capabilities of one of the solution methods.

NOMENCLATURE

$\overline{A}_{g\ell}$ = surface area between vapor and liquid phase per unit volume

$\overline{A}_{wg}$ = surface area of vapor phase in contact with the wall per unit volume

$\overline{A}_{w\ell}$ = surface area of liquid phase in contact with the wall per unit volume

$B_{g\ell}$ = friction coefficient between vapor and liquid phases

B_{wg} = stationary form and viscous drag between wall and vapor phase

$B_{w\ell}$ = stationary form and viscous drag between wall and liquid phase

F = unspecified forces in the momentum equations

F_{gs} = fraction of the vapor phase which is at saturation

$F_{\ell s}$ = fraction of the liquid phase which is at saturation

g_x = axial component of acceleration due to gravity

h_{gs} = enthalpy of saturated vapor

$h_{\ell s}$ = enthalpy of saturated liquid

$\dot{m}$ = rate of vapor generation per unit volume

$\dot{m}_{\Delta P}$ = rate of vapor generation per unit volume due to pressure changes

$\dot{m}_{\Delta T}$ = rate of vapor generation per unit volume due to temperature changes

P = pressure

$\dot{q}^g$ = heat flux to vapor phase per unit volume

$\dot{q}^\ell$ = heat flux to liquid phase per unit volume

S_{gs} = entropy of saturated vapor

$S_{\ell s}$ = entropy of saturated liquid

T_s = saturation temperature

u_g = internal energy of vapor phase

u_ℓ = internal energy of liquid phase

u_{gs} = internal energy of saturated vapor

$u_{\ell s}$ = internal energy of saturated liquid

v^g = velocity of vapor phase

v^ℓ = velocity of liquid phase

$\hat{v}$ = intrinsic velocity

α = vapor volume fraction

α^ℓ = liquid volume fraction ($\alpha^\ell = 1-\alpha$)

ρ_g = density of vapor phase

ρ_ℓ = density of liquid phase

ρ_{gs} = density of vapor phase at saturation pressure

$\rho_{\ell s}$ = density of liquid phase at saturation pressure

Δt = time step

Δx = spatial mesh increment.

CONTENTS

FIGURES

NUMERICAL METHODS FOR SOLVING THE GOVERNING EQUATIONS FOR A SERIATED CONTINUUM

I. INTRODUCTION

The ability to compute hydraulic transients is required to accurately predict the phenomena of a loss-of-coolant accident (LOCA) in a nuclear reactor. Since the reactor coolant could be a two-phase mixture during at least part of the LOCA, a possibility exists for two phases with unequal velocities or unequal temperatures or both. Consequently, the homogeneous fluid models used in current reactor system codes may prove inadequate in many cases. The desire to more accurately predict two-phase flow behavior has resulted in investigations into the feasibility of computing both unequal phase velocities and unequal phase temperatures (References 1 and 2, for example).

Solbrig and Hughes[3] describe governing equations for a seriated continuum for the unequal velocity, equal temperature (UVET) case. Other authors have described equations for the unequal velocity, unequal temperature (UVUT) case (Reference 1, for example).

This report documents finite difference forms of the UVET equations, a related set of UVUT equations, and two methods developed for solving the resulting systems of simultaneous nonlinear equations. Both methods described are related to the Implicit Continuous-fluid Eulerian (ICE) method as reported in Reference 4. One of the methods, called ICE-PF, is related to the Implicit Multifield Flows (IMF) scheme[1] used in the KACHINA code[5] and extends IMF to the case of two completely compressible phases. The other technique is called the Seriated Continuum Implicit (SCIMP) method and includes an implicit treatment of momentum flux. In addition, results from the experimental Seriated Tube code (STUBE) are presented to illustrate the capabilities of the SCIMP method.

Among the features of these solution techniques are:

(1) A high degree of implicitness allowing applicability to all flow speeds

(2) Compressibility of both phases

(3) Mass transfer between phases

(4) Implicit coupling of the phases through the interphase friction and the mass exchange mechanisms.

II. GOVERNING EQUATIONS

The description of a two-component seriated continuum requires five field equations in the case of UVET flows and six field equations in the case of UVUT flows. In each case the requirement is a continuity equation for each phase and a momentum equation for each phase. In addition, equations that govern the conservation of energy for the fluid are required. In the case of UVET theory there is a single equation for the conservation of the average energy of the system, and in the UVUT theory there is an energy equation for each of the phases. In addition to the field equations, there are equations of state for all of the components and various other constitutive equations.

The systems of field equations used for both the UVET model and the UVUT model are presented in this section. The letters ℓ and g are used as subscripts and superscripts referring to the liquid and vapor (gas) phases, respectively. Other nomenclature is listed in the appendix.

1. CONTINUITY EQUATIONS

The gas phase continuity equation is

$$\frac{\partial}{\partial t}(\alpha\rho_g) + \frac{\partial}{\partial x}(\alpha\rho_g v^g) = \dot{m} \tag{1}$$

and the liquid phase continuity equation is

$$\frac{\partial}{\partial t}(\alpha^\ell\rho_\ell) + \frac{\partial}{\partial x}(\alpha^\ell\rho_\ell v^\ell) = -\dot{m}. \tag{2}$$

2. MOMENTUM EQUATIONS

The gas phase momentum equation is

$$\frac{\partial}{\partial t}(\alpha\rho_g v^g) + \frac{\partial}{\partial x}(\alpha\rho_g v^g v^g) = -\alpha\frac{\partial p}{\partial x} + \dot{m}\hat{v}$$

$$-\bar{A}_{g\ell}B_{g\ell}(v^g - v^\ell) - \bar{A}_{wg}B_{wg}v^g + \alpha\rho_g g_x + F \tag{3}$$

and the liquid phase momentum equation is

$$\frac{\partial}{\partial t}(\alpha^{\ell}\rho_{\ell}v^{\ell}) + \frac{\partial}{\partial x}(\alpha^{\ell}\rho_{\ell}v^{\ell}v^{\ell}) = -\alpha^{\ell}\frac{\partial p}{\partial x} - \dot{m}\hat{v}$$

$$- \bar{A}_{g\ell}B_{g\ell}(v^{\ell} - v^{g}) - \bar{A}_{w\ell}B_{w\ell}v^{\ell} + \alpha^{\ell}\rho_{\ell}g_{x} - F. \tag{4}$$

The "F term" in these equations represents terms such as transient flow forces or added mass effects that are often flow regime- or geometry-dependent. This term is not necessary for a description of the basic numerical schemes and is not considered in this report.

3. ENERGY EQUATIONS

The internal energy equations for UVUT flows, written in nonconservative form, are

$$\alpha\rho_{g}\frac{\partial u_{g}}{\partial t} + \alpha\rho_{g}v^{g}\frac{\partial u_{g}}{\partial x} = \dot{m}\left(u_{gs} - u_{g} + \frac{p}{\rho_{gs}}\right)$$

$$+ \dot{q}^{g} - p\left[\frac{\partial \alpha}{\partial t} + \frac{\partial}{\partial x}(\alpha v^{g})\right] \tag{5}$$

and

$$\alpha^{\ell}\rho_{\ell}\frac{\partial u_{\ell}}{\partial t} + \alpha^{\ell}\rho_{\ell}v^{\ell}\frac{\partial u_{\ell}}{\partial x} = -\dot{m}\left(u_{\ell s} - u_{\ell} + \frac{p}{\rho_{\ell s}}\right)$$

$$+ \dot{q}^{\ell} - p\left[\frac{\partial \alpha^{\ell}}{\partial t} + \frac{\partial}{\partial x}(\alpha^{\ell}v^{\ell})\right]. \tag{6}$$

In the UVET model the equation for the mixture internal energy is

$$(\alpha\rho_{g} + \alpha^{\ell}\rho_{\ell})\frac{\partial u_{m}}{\partial t} + (\alpha\rho_{g}v^{g} + \alpha^{\ell}\rho_{\ell}v^{\ell})\frac{\partial u_{m}}{\partial x} = \dot{q} - p\frac{\partial}{\partial x}(\alpha v^{g} + \alpha^{\ell}v^{\ell}). \tag{6a}$$

4. EQUATIONS OF STATE

In UVUT flows and in single-phase flows the thermodynamic densities of the phases are determined as functions of the pressure and internal energies from the equations of state

$$\rho_g = \rho_g (P, u_g) \tag{7}$$

and/or

$$\rho_\ell = \rho_\ell (P, u_\ell). \tag{8}$$

For UVET flows, the state properties in the two-phase region are functions of pressure alone; so Equations (7) and (8) are replaced by

$$\rho_g = \rho_{gs}(P) \tag{7a}$$

and

$$\rho_\ell = \rho_{\ell s}(P) \tag{8a}$$

respectively.

5. CONSTITUTIVE FLASHING RATE EQUATION

The rate of net vapor production $\dot{m}$ appearing in these equations is assumed to be linearly partitioned into two parts: the mass transfer rate due to pressure change $\dot{m}_{\Delta P}$ and the mass transfer rate due to temperature differences $\dot{m}_{\Delta T}$ as

$$\dot{m} = \dot{m}_{\Delta P} + \dot{m}_{\Delta T}.$$

The model used for $\dot{m}_{\Delta P}$ in the STUBE code is

$$\dot{m}_{\Delta P} = -T_s \frac{\left[F_{\ell s}\alpha^\ell \rho_\ell \left(\frac{\partial S_{\ell s}}{\partial t} + v^\ell \frac{\partial S_{\ell s}}{\partial x}\right) + F_{gs}\,\alpha \rho_g \left(\frac{\partial S_{gs}}{\partial t} + v^g \frac{\partial S_{gs}}{\partial x}\right)\right]}{h_{gs} - h_{\ell s}}. \tag{9}$$

This model is similar to those derived in References 6 and 7.

If the system is assumed to be adiabatic, the UVUT theory can be degenerated to UVET theory by setting the phase energies to the saturation values at the prevailing pressure and setting $F_{\ell s} = F_{gs} = 1$ in Equation (9). In this case, Equation (9) is a combination of the mixture energy equation and the continuity equations. This equation replaces the mixture energy equation, Equation (6a), as a field equation.

6. ADDITIONAL RELATIONS

The additional relations needed to complete the equation sets are:

(1) Equations of state for the thermodynamic energies along the phase boundary in the UVET case

$$u_g = u_{gs}(P)$$

and

$$u_\ell = u_{\ell s}(P)$$

(2) Summation of the volume fractions

$$\alpha + \alpha^\ell = 1.$$

Constitutive equations are required to describe mass, momentum, and energy exchange between phases and between the fluid and adjacent surfaces. Examples of correlations and models used in these equations can be found in Solbrig et al[8].

III. FINITE DIFFERENCE EQUATIONS

In order to solve a transient flow problem described by either UVUT or UVET field equations with appropriate initial and boundary conditions on an interval, $0 \leqslant x \leqslant L$, the field equations are replaced by a set of finite difference equations. The interval, $0 \leqslant x \leqslant L$, is partitioned into N computational cells of equal length Δx so that $L = N\Delta x$. The finite difference equations are obtained by centrally differencing the field equations on a staggered mesh. The difference equations are presented for equal cell sizes. The equations for unequal spatial increments are a straightforward generalization of the equal increment equations.

A typical computational cell for the continuity and energy equations is shown below.

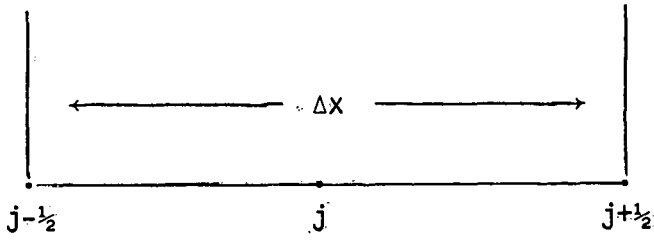

The j denotes $x_j = j\Delta x - \frac{1}{2}\Delta x$, which is the x-coordinate at the center of the jth cell. In the difference equations, subscripts are used to refer to the spatial coordinate, while superscripts refer to the time level. For example, the thermodynamic density of the gas at the cell center at time, $(t_o + n\Delta t)$, is denoted as

$$(\rho_g)^n_j \equiv \rho_g((j-\tfrac{1}{2})\Delta x,\ t_o + n\Delta t).$$

The momentum equations are differenced on a computational cell which is offset one-half cell. A typical computational cell for the momentum equation is shown below. The gas velocity at the center of this cell is denoted by $(v_g)_{j+\frac{1}{2}}$.

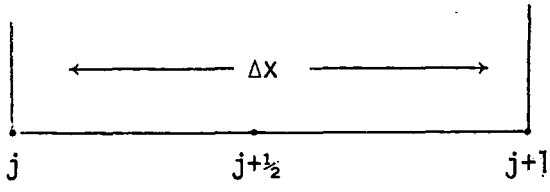

That is, pressure, void fraction, densities, and energies are calculated at cell centers, and velocities are calculated at cell boundaries. Whenever a quantity is required at a point where it is not determined by a finite difference field equation or by a constitutive equation, appropriate averages are used. For example

$$(\rho_g)^n_{j+\frac{1}{2}} \equiv \tfrac{1}{2}[(\rho_g)^n_j + (\rho_g)^n_{j+1}] \text{ and } (v^g)^n_j \equiv \tfrac{1}{2}[(v^g)^n_{j-\frac{1}{2}} + (v^g)^n_{j+\frac{1}{2}}].$$

1. CONTINUITY EQUATIONS

The finite difference forms of the continuity equations used in the SCIMP and ICE-PF methods are

$$\frac{(\alpha\rho_g)_j^{n+1} - (\alpha\rho_g)_j^n}{\Delta t} + \frac{(\alpha\rho_g v^g)_{j+\frac{1}{2}}^{n+1} - (\alpha\rho_g v^g)_{j-\frac{1}{2}}^{n+1}}{\Delta x} = \dot{m}_j^{n+1} \tag{10}$$

and

$$\frac{(\alpha^\ell\rho_\ell)_j^{n+1} - (\alpha^\ell\rho_\ell)_j^n}{\Delta t} + \frac{(\alpha^\ell\rho_\ell v^\ell)_{j+\frac{1}{2}}^{n+1} - (\alpha^\ell\rho_\ell v^\ell)_{j-\frac{1}{2}}^{n+1}}{\Delta x} = -\dot{m}_j^{n+1}. \tag{11}$$

For some flows the centered difference convective fluxes are replaced by donor cell fluxes in the ICE-PF method. The donor cell flux $\langle Qv \rangle_{j+\frac{1}{2}}$ of a quantity Q is defined by

$$\langle Qv \rangle_{j+\frac{1}{2}} = \begin{cases} Q_j\, v_{j+\frac{1}{2}} & \text{if} \quad v_{j+\frac{1}{2}} \geq 0 \\ Q_{j+1}\, v_{j+\frac{1}{2}} & \text{if} \quad v_{j+\frac{1}{2}} < 0. \end{cases}$$

Whenever the donor cell technique is used, the finite difference forms of the continuity equations are

$$\frac{(\alpha\rho_g)_j^{n+1} - (\alpha\rho_g)_j^n}{\Delta t} + \frac{\langle \alpha\rho_g v^g \rangle_{j+\frac{1}{2}}^{n+1} - \langle \alpha\rho_g v^g \rangle_{j-\frac{1}{2}}^{n+1}}{\Delta x} = \dot{m} \tag{10a}$$

and

$$\frac{(\alpha^\ell\rho_\ell)_j^{n+1} - (\alpha^\ell\rho_\ell)_j^n}{\Delta t} + \frac{\langle \alpha^\ell\rho_\ell v^\ell \rangle_{j+\frac{1}{2}}^{n+1} - \langle \alpha^\ell\rho_\ell v^\ell \rangle_{j-\frac{1}{2}}^{n+1}}{\Delta x} = -\dot{m}. \tag{11a}$$

2. MOMENTUM EQUATIONS

The finite difference forms of the momentum equations used for the SCIMP method are

$$\frac{(\alpha\rho_g v^g)^{n+1}_{j+\frac{1}{2}} - (\alpha\rho_g v^g)^{n}_{j+\frac{1}{2}}}{\Delta t} + \frac{(\alpha\rho_g v^g v^g)^{n+1}_{j+1} - (\alpha\rho_g v^g v^g)^{n+1}_{j}}{\Delta x} =$$

$$-\alpha^{n+1}_{j+\frac{1}{2}} \frac{p^{n+1}_{j+1} - p^{n+1}_{j}}{\Delta x} + \dot{m}^{n+1}_{j+\frac{1}{2}} \hat{v}^{n+1}_{j+\frac{1}{2}} - (\bar{A}_{g\ell} B_{g\ell})^{n+1}_{j+\frac{1}{2}} (v^g - v^\ell)^{n+1}_{j+\frac{1}{2}}$$

$$- (\bar{A}_{wg} B_{wg})^{n+1}_{j+\frac{1}{2}} (v^g)^{n+1}_{j+\frac{1}{2}} + (\alpha\rho_g)^{n+1}_{j+\frac{1}{2}} g_x \qquad (12)$$

and

$$\frac{(\alpha^\ell\rho_\ell v^\ell)^{n+1}_{j+\frac{1}{2}} - (\alpha^\ell\rho_\ell v^\ell)^{n}_{j+\frac{1}{2}}}{\Delta t} + \frac{(\alpha^\ell\rho_\ell v^\ell v^\ell)^{n+1}_{j+1} - (\alpha^\ell\rho_\ell v^\ell v^\ell)^{n+1}_{j}}{\Delta x} =$$

$$-(\alpha^\ell)^{n+1}_{j+\frac{1}{2}} \frac{p^{n+1}_{j+1} - p^{n+1}_{j}}{\Delta x} - \dot{m}^{n+1}_{j+\frac{1}{2}} \hat{v}^{n+1}_{j+\frac{1}{2}} - (\bar{A}_{g\ell} B_{g\ell})^{n+1}_{j+\frac{1}{2}} (v^\ell - v^g)^{n+1}_{j+\frac{1}{2}}$$

$$- (\bar{A}_{w\ell} B_{w\ell})^{n+1}_{j+\frac{1}{2}} (v^\ell)^{n+1}_{j+\frac{1}{2}} + (\alpha^\ell\rho_\ell)^{n+1}_{j+\frac{1}{2}} g_x . \qquad (13)$$

For the ICE-PF method, the momentum equations are written in nonconservative form with the momentum flux terms differenced at the old time level ($t_o + n\Delta t$). The momentum equations used for the ICE-PF method are

$$(\alpha\rho_g)^{n}_{j} \frac{(v^g)^{n+1}_{j+\frac{1}{2}} - (v^g)^{n}_{j+\frac{1}{2}}}{\Delta t} + (\alpha\rho_g v^g)^{n}_{j+\frac{1}{2}} \frac{(v^g)^{n}_{j+1} - (v^g)^{n}_{j}}{\Delta x} =$$

$$- \alpha^{n+1}_{j+\frac{1}{2}} \frac{p^{n+1}_{j+1} - p^{n+1}_{j}}{\Delta x} + \dot{m}^{n+1}_{j+\frac{1}{2}} \left(\hat{v}^{n+1}_{j+\frac{1}{2}} - (v^g)^{n+1}_{j+\frac{1}{2}} \right)$$

$$- (\bar{A}_{g\ell} B_{g\ell})^{n+1}_{j+\frac{1}{2}} (v^g - v^\ell)^{n+1}_{j+\frac{1}{2}} - (A_{wg} B_{wg})^{n+1}_{j+\frac{1}{2}} (v^g)^{n+1}_{j+\frac{1}{2}} + (\alpha\rho_g)^{n+1}_{j+\frac{1}{2}} g_x \qquad (12a)$$

and

$$(\alpha^{\ell}\rho^{\ell})^{n}_{j}\frac{(v^{\ell})^{n+1}_{j+\frac{1}{2}}-(v^{\ell})^{n}_{j+\frac{1}{2}}}{\Delta t}+(\alpha^{\ell}\rho_{\ell}v^{\ell})^{n}_{j+\frac{1}{2}}\frac{(v^{\ell})^{n}_{j+1}-(v^{\ell})^{n}_{j}}{\Delta x}=$$

$$-(\alpha^{\ell})^{n+1}_{j+\frac{1}{2}}\frac{p^{n+1}_{j+1}-p^{n+1}_{j}}{\Delta x}-\dot{m}^{n+1}_{j+\frac{1}{2}}\left(\hat{v}^{n+1}_{j+\frac{1}{2}}-(v^{\ell})^{n+1}_{j+\frac{1}{2}}\right)$$

$$-(\overline{A}_{g\ell}B_{g\ell})^{n+1}_{j+\frac{1}{2}}(v^{\ell}-v^{g})^{n+1}_{j+\frac{1}{2}}-(A_{w\ell}B_{w\ell})(v^{\ell})^{n+1}_{j+\frac{1}{2}}+(\alpha^{\ell}\rho_{\ell})^{n+1}_{j+\frac{1}{2}}g_{x}\ . \tag{13a}$$

3. ENERGY EQUATIONS

For UVUT flows and single-phase flows, the finite difference forms of the energy equations are

$$(\alpha\rho_{g})^{n}_{j}\frac{(u_{g})^{n+1}_{j}-(u_{g})^{n}_{j}}{\Delta t}+(\alpha\rho_{g}v^{g})^{n}_{j}\frac{(u_{g})^{n+1}_{j+\frac{1}{2}}-(u_{g})^{n+1}_{j+\frac{1}{2}}}{\Delta x}=$$

$$-p^{n}_{j}\left[\frac{\alpha^{n}_{j}-\alpha^{n-1}_{j}}{\Delta t}+\frac{(\alpha v^{g})^{n}_{j+\frac{1}{2}}-(\alpha v^{g})^{n}_{j-\frac{1}{2}}}{\Delta x}\right]+(\dot{q}^{g})^{n}_{j}$$

$$+(\dot{m})^{n}_{j}\left(u_{gs}-u_{g}+\frac{p}{\rho_{gs}}\right)^{n}_{j} \tag{14}$$

and

$$(\alpha^{\ell}\rho_{\ell})^{n}_{j}\frac{(u_{\ell})^{n+1}_{j}-(u_{\ell})^{n}_{j}}{\Delta t}+(\alpha^{\ell}\rho_{\ell}v^{\ell})^{n}_{j}\frac{(u_{\ell})^{n+1}_{j+\frac{1}{2}}-(u_{\ell})^{n+1}_{j-\frac{1}{2}}}{\Delta x}=$$

$$-p^{n}_{j}\left[\frac{(\alpha^{\ell})^{n}_{j}-(\alpha^{\ell})^{n-1}}{\Delta t}+\frac{(\alpha^{\ell}v^{\ell})^{n}_{j+\frac{1}{2}}-(\alpha^{\ell}v^{\ell})^{n}_{j-\frac{1}{2}}}{\Delta x}\right]+(\dot{q}^{\ell})^{n}_{j}$$

$$-(\dot{m})^{n}_{j}\left(u_{\ell s}-u_{\ell}+\frac{p}{\rho_{\ell s}}\right)^{n}_{j}\ . \tag{15}$$

When these forms of the finite difference energy equations are used for computation in two-phase flow situations, the vapor superheats unrealistically, particularly when there is mass exchange between the phases. This superheating is due, in part, to numerical error that is eliminated by a modification of Equations (14) and (15).

The modification of the energy equations is accomplished by substituting a continuity equation into the right side of each of Equations (14) and (15). The vapor continuity equation, Equation (1), is written in the form

$$\frac{\partial \alpha}{\partial t} + \frac{\partial (\alpha v^g)}{\partial x} = \frac{\dot{m}}{\rho_g} - \frac{\alpha}{\rho_g}\left[\frac{\partial \rho_g}{\partial t} + v^g \frac{\partial \rho_g}{\partial x}\right].$$

This form of the continuity equation is then finite differenced as

$$\frac{\alpha_j^n - \alpha_j^{n-1}}{\Delta t} + \frac{(\alpha v^g)^n_{j+\frac{1}{2}} - (\alpha v^g)^n_{j-\frac{1}{2}}}{\Delta x} =$$

$$\frac{\dot{m}_j^n}{(\rho_g)_j^n} - \frac{\alpha_j^n}{(\rho_g)_j^n}\left[\frac{(\rho_g)_j^n - (\rho_g)_j^{n-1}}{\Delta t} + (v^g)_j^n \frac{(\rho_g)^n_{j+\frac{1}{2}} - (\rho_g)^n_{j-\frac{1}{2}}}{\Delta x}\right].$$

Substituting into Equation (14) gives

$$(\alpha\rho_g)_j^n \frac{(u_g)_j^{n+1} - (u_g)_j^n}{\Delta t} + (\alpha\rho_g v^g)_j^n \frac{(u_g)^{n+1}_{j+\frac{1}{2}} - (u_g)^{n+1}_{j-\frac{1}{2}}}{\Delta x} =$$

$$\frac{(p\alpha)_j^n}{(\rho_g)_j^n}\left[\frac{(\rho_g)_j^n - (\rho_g)_j^{n-1}}{\Delta t} + (v^g)_j^n \frac{(\rho_g)^n_{j+\frac{1}{2}} - (\rho_g)^n_{j-\frac{1}{2}}}{\Delta x}\right] + (\dot{q}^g)_j^n$$

$$+ (\dot{m}p)_j^n \left(\frac{1}{\rho_{gs}} - \frac{1}{\rho_g}\right)_j^n + \dot{m}_j^n (u_{gs} - u_g)_j^n . \qquad (14a)$$

The liquid energy equation, Equation (15) is modified in an analogous manner to give

$$(\alpha^\ell\rho_\ell)_j^n \frac{(u_\ell)_j^{n+1} - (u_\ell)_j^n}{\Delta t} + (\alpha^\ell\rho_\ell v^\ell)_j^n \frac{(u_\ell)^{n+1}_{j+\frac{1}{2}} - (u_\ell)^{n+1}_{j-\frac{1}{2}}}{\Delta x} =$$

$$\frac{(p\alpha^\ell)_j^n}{(\rho_\ell)_j^n}\left[\frac{(\rho_\ell)_j^n - (\rho_\ell)_j^{n-1}}{\Delta t} + (v^\ell)_j^n \frac{(\rho_\ell)^n_{j+\frac{1}{2}} - (\rho_\ell)^n_{j-\frac{1}{2}}}{\Delta x}\right] + (\dot{q}^\ell)_j^n$$

$$+ (\dot{m}p)_j^n \left(\frac{1}{\rho_{\ell s}} - \frac{1}{\rho_\ell}\right)_j^n - \dot{m}_j^n (u_{\ell s} - u_\ell)_j^n . \qquad (15a)$$

Equations (14a) and (15a) are forms of the energy equations used for computational purposes.

For UVET flow, the finite difference form of the combined energy, continuity equation is

$$\frac{-(T_s)_j^{n+1}}{(h_{gs})_j^{n+1} - (h_{\ell s})_j^{n+1}} \left[(F_{\ell s}\alpha^{\ell}\rho_{\ell})_j^{n+1} \left(\frac{(S_{\ell s})_j^{n+1} - (S_{\ell s})_j^{n}}{\Delta t} + (v^{\ell})_j^{n+1} \frac{(S_{\ell s})_{j+\frac{1}{2}}^{n+1} - (S_{\ell s})_{j-\frac{1}{2}}^{n+1}}{\Delta x} \right) + (F_{gs}\alpha\rho_g)_j^{n+1} \left(\frac{(S_{gs})_j^{n+1} - (S_{gs})_j^{n}}{\Delta t} + (v^{g})_j^{n+1} \frac{(S_{gs})_{j+\frac{1}{2}}^{n+1} - (S_{gs})_{j-\frac{1}{2}}^{n+1}}{\Delta x} \right) \right] = (\dot{m}_{\Delta P})_j^{n+1} . \tag{16}$$

4. EQUATIONS OF STATE

For UVUT flows and single-phase flows, the thermodynamic densities of the phases

$$(\rho_g)_j^{n+1} = \rho_g \left(p_j^{n+1}, (u_g)_j^{n+1}\right) \tag{17}$$

and

$$(\rho_{\ell})_j^{n+1} = \rho_{\ell} \left(p^{n+1}, (u_{\ell})_j^{n+1}\right) \tag{18}$$

are determined from the equations of state. For UVET flows, the densities in the two-phase region are functions of pressure alone. The appropriate equations of state are

$$(\rho_g)_j^{n+1} = \rho_{gs}(p_j^{n+1}) \tag{19}$$

and

$$(\rho_{\ell})_j^{n+1} = \rho_{\ell s}(p_j^{n+1}) . \tag{20}$$

Also, in the UVET case, the energies in the two-phase region are saturation values. These energies are obtained from the state relationships

$$(u_g)_j^{n+1} = u_{gs}(P_j^{n+1}) \tag{21}$$

and

$$(u_\ell)_j^{n+1} = u_{\ell s}(P_j^{n+1}) \ . \tag{22}$$

5. BOUNDARIES

In addition to the finite difference field equations given in the preceding sections, formulation of a boundary value problem requires information at the end points of the interval, $0 \leqslant x \leqslant L$. Values for some of the variables may be constrained at the boundary points for a particular physical problem. The values for those variables not specified by physical constraints are obtained by solving finite difference equations written over a half cell. The computational cell used at x=0 is shown below.

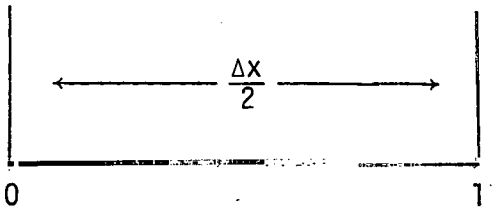

The continuity equation for the vapor phase is finite differenced at x=0 using a forward spatial step as follows

$$\frac{(\alpha\rho_g)_0^{n+1} - (\alpha\rho_g)_0^n}{\Delta t} + \frac{(\alpha\rho_g v^g)_1^{n+1} - (\alpha\rho_g v^g)_0^{n+1}}{(\Delta x/2)} = \dot{m}_0^{n+1} . \tag{23}$$

At the end point $L = N\Delta x$ the half-size computational cell used is shown below.

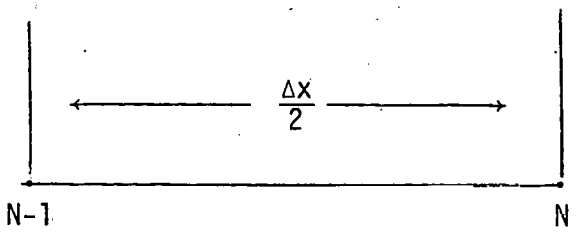

The continuity equation for the vapor phase is differenced at x=L using a backward spatial step as follows

$$\frac{(\alpha\rho_g)_N^{n+1} - (\alpha\rho_g v^g)_N^n}{\Delta t} + \frac{(\alpha\rho_g v^g)_N^{n+1} - (\alpha\rho_g v^g)_{N-1}^{n+1}}{(\Delta x/2)} = \dot{m}_N^{n+1} \quad . \tag{24}$$

The remaining equations for both phases are differenced in an analogous manner using a forward or backward spatial difference as appropriate.

IV. SOLUTION OF FINITE DIFFERENCE EQUATIONS

The finite difference equations above are systems of simultaneous nonlinear equations solved for the problem variables at time $(n+1)\Delta t$ in terms of the values at time $n\Delta t$. The SCIMP and ICE-PF methods for solving these systems of equations are described in this section. Both methods are based on the ICE method for homogeneous flows reported in Reference 4 and represent extensions of the ICE method to two-phase flows.

1. THE SERIATED CONTINUUM IMPLICIT METHOD

The SCIMP method is characterized by replacing the vapor continuity equation with an appropriately formulated pressure equation. The derivation of the pressure equation involves combining the phase continuity equations, the phase momentum equations, state equations, and the constitutive flashing rate equation.

First the continuity equations, Equations (1) and (2), are written as

$$\rho_g \frac{\partial \alpha}{\partial t} + \alpha \frac{\partial \rho_g}{\partial t} + \frac{\partial}{\partial x}(\alpha \rho_g v^g) = \dot{m} \tag{1a}$$

and

$$\rho_\ell \frac{\partial \alpha^\ell}{\partial t} + \alpha^\ell \frac{\partial \rho_\ell}{\partial t} + \frac{\partial}{\partial x}(\alpha^\ell \rho_\ell v^\ell) = -\dot{m} . \tag{2a}$$

Equations (1a) and (2a) are multiplied by ρ_ℓ and ρ_g, respectively, and then added to eliminate the $\partial\alpha/\partial t$ terms

$$\rho_\ell \alpha \frac{\partial \rho_g}{\partial t} + \rho_g \alpha^\ell \frac{\partial \rho_\ell}{\partial t} + \rho_\ell \frac{\partial}{\partial x}(\alpha \rho_g v^g) + \rho_g \frac{\partial}{\partial x}(\alpha^\ell \rho_\ell v^\ell) = (\rho_g - \rho_\ell)\dot{m}. \tag{25}$$

Now the state equations, Equations (7) through (8a), are differentiated with respect to time, giving

$$\frac{\partial \rho_g}{\partial t} = \frac{\partial \rho_g}{\partial p}\frac{\partial p}{\partial t} + \frac{\partial \rho_g}{\partial u_g}\frac{\partial u_g}{\partial t} \tag{26}$$

and

$$\frac{\partial \rho_\ell}{\partial t} = \frac{\partial \rho_\ell}{\partial p}\frac{\partial p}{\partial t} + \frac{\partial \rho_\ell}{\partial u_\ell}\frac{\partial u_\ell}{\partial t} \tag{27}$$

for UVUT flows and

$$\frac{\partial \rho_g}{\partial t} = \frac{\partial \rho_g}{\partial P} \frac{\partial P}{\partial t} \tag{28}$$

and

$$\frac{\partial \rho_\ell}{\partial t} = \frac{\partial \rho_\ell}{\partial P} \frac{\partial P}{\partial t} \tag{29}$$

for UVET flows.

Depending on the flow model, UVET or UVUT, the appropriate state equations, Equations (26) through (29), are used to eliminate $\frac{\partial \rho_g}{\partial t}$ and $\frac{\partial \rho_\ell}{\partial t}$ in Equation (25).

The resulting equation for the UVUT flow model is

$$\left(\alpha\rho_\ell \frac{\partial \rho_g}{\partial p} + \alpha^\ell \rho_g \frac{\ell}{\partial p}\right) \frac{\partial P}{\partial t} + \rho_\ell \alpha \frac{\partial \rho_g}{\partial u_g} \frac{\partial u_g}{\partial t}$$

$$+ \rho_g \alpha^\ell \frac{\partial \rho_\ell}{\partial u_\ell} \frac{\partial u_\ell}{\partial t} + \rho_\ell \frac{\partial}{\partial x}(\alpha \rho_g v^g) + \rho_g \frac{\partial}{\partial x}(\alpha^\ell \rho_\ell v^\ell)$$

$$= (\rho_g - \rho_\ell)\, \dot{m}. \tag{30}$$

In the UVET case, the terms $\rho_\ell \alpha \frac{\partial \rho_g}{\partial u_g} \frac{\partial u_g}{\partial t}$ and $\rho_g \alpha^\ell \frac{\partial \rho_\ell}{\partial u_\ell} \frac{\partial u_\ell}{\partial t}$ do not appear in Equation (30). Equation (30) is now finite differenced as follows

$$\left[(\rho_\ell \alpha)_j^{n+1} \left(\frac{\partial \rho_g}{\partial P}\right)_j^n + (\rho_g \alpha^\ell)_j^{n+1} \left(\frac{\partial \rho_\ell}{\partial P}\right)_j^n\right] \frac{P_j^{n+1} - P_j^n}{\Delta t}$$

$$+ (\rho_\ell \alpha)_j^{n+1} \left(\frac{\partial \rho_g}{\partial u_g}\right)_j^n \frac{(u_g)_j^{n+1} - (u_g)^n}{\Delta t} + (\rho_g \alpha^\ell)_j^{n+1} \left(\frac{\partial \rho_\ell}{\partial u_\ell}\right)_j^n \frac{(u_\ell)_j^{n+1} - (u_\ell)_j^n}{\Delta t}$$

$$+ (\rho_\ell)_j^{n+1} \frac{(\alpha \rho_g v^g)_{j+\frac{1}{2}}^{n+1} - (\alpha \rho_g v^g)_{j-\frac{1}{2}}^{n+1}}{\Delta x} + (\rho_g)_j^{n+1} \frac{(\alpha^\ell \rho_\ell v^\ell)_{j+\frac{1}{2}}^{n+1} - (\alpha^\ell \rho_\ell v^\ell)_{j-\frac{1}{2}}^{n+1}}{\Delta x}$$

$$= (\rho_g - \rho_\ell)_j^{n+1} \dot{m}_j^{n+1}. \tag{31}$$

Equation (10) is replaced by Equation (31) in the system of equations to be solved.

The explicit energy equations, Equations (14a) and (15a), are solved first; then the remaining equations are solved iteratively until the pressure is converged. The variables, other than energy, for a UVUT problem are determined by iteratively solving:

(1) The pressure equation, Equation (31), for P

(2) The state equations for the thermodynamic densities, ρ_g and ρ_ℓ

(3) The momentum equations, Equations (12) and (13), for v^g and v^ℓ

(4) The liquid continuity equation, Equation (11), for the product $(\alpha^\ell \rho_\ell)$.

The void fraction α is computed by dividing the product $(\alpha^\ell \rho_\ell)$ by the liquid thermodynamic density and subtracting the result from one.

With the exception of the pressure equation, the finite difference equations, as presented, are in a form suitable for numerical solution. For the iterative procedure, the pressure equation, Equation (31), is further modified. First the vapor momentum equation, Equation (12), is solved algebraically for $(\alpha\rho_g v^g)^{n+1}_{j+\frac{1}{2}}$ and the liquid momentum equation, Equation (13), is solved for $(\alpha^\ell \rho_\ell v^\ell)^{n+1}_{j+\frac{1}{2}}$. Then the momentum equations are differenced about the point $j\Delta x$ (the left boundary of cell j) and the resulting equations solved for $(\alpha\rho_g v^g)^{n+1}_{j-\frac{1}{2}}$, and $(\alpha^\ell \rho_\ell v^\ell)^{n+1}_{j-\frac{1}{2}}$. The expressions obtained for $(\alpha\rho_g v^g)^{n+1}_{j\pm\frac{1}{2}}$ and for $(\alpha^\ell \rho_\rho v^\ell)^{n+1}_{j\pm\frac{1}{2}}$ are then substituted into Equation (31). This results in feedback of the velocity field computation into the pressure field computation.

Experience solving depressurization problems with mass exchange between the phases, using the technique discussed above, indicates the pressure computation to be a sensitive function of $\dot{m}_{\Delta p}$. This sensitivity requires that the effect of phase changes due to pressure changes be fed back directly into the pressure field computation. For the pressure equation, the spatial dependence is dropped from the constitutive flashing rate equation, Equation (9), and the resulting equation is written as

$$\dot{m}_{\Delta p} = - \frac{T_s}{h_{gs} - h_{\ell s}} \left(F_{gs} \alpha \rho_g \frac{\partial s_{gs}}{\partial p} + \Gamma_{\ell s} \alpha^\ell \rho_\ell \frac{\partial s_{\ell s}}{\partial p} \right) \frac{\partial p}{\partial t} \quad . \tag{32}$$

The finite difference form of Equation (32) is substituted into the finite differenced pressure equation, Equation (31), giving the final form of the iteration pressure equation, Equation (33). The superscripts r and r+1 denote quantities at old and new iteration values at time $(n+1)\Delta t$.

Iteration Pressure Equation

$$P_{j-1}^{r+1}\left(\frac{\Delta t}{\Delta x}\right)^2\left((\rho_\ell)_j^r\,\alpha_{j-\frac{1}{2}}^r+(\rho_g)_j^r\,(\alpha_\ell)_{j-\frac{1}{2}}^r\right)+P_{j+1}^{r+1}\left(\frac{\Delta t}{\Delta x}\right)^2\left((\rho_\ell)_j^r\,\alpha_{j+\frac{1}{2}}^r+(\rho_g)_j^r\,(\alpha^\ell)_{j+\frac{1}{2}}^r\right)$$

$$+P_j^{r+1}\Bigg[-2\left(\frac{\Delta t}{\Delta x}\right)^2\left((\rho_\ell\alpha)_j^r+(\rho_g\alpha^\ell)_j^r\right)-\left((\rho_\ell\alpha)_j^r\left(\frac{\partial\rho_g}{\partial p}\right)_j+(\rho_g\alpha^\ell)_j^r\left(\frac{\partial\rho_\ell}{\partial p}\right)_j\right)$$

$$-\frac{(\rho_\ell-\rho_g)_j^r\,(T_s)_j^r}{(h_{gs}-h_{\ell s})_j^r}\left((F_{gs})_j^{n+1}(\alpha\rho_g)_j^r\left(\frac{\partial S_{gs}}{\partial p}\right)_j+(F_{\ell s})_j^{n+1}(\alpha^\ell\rho_\ell)_j^r\left(\frac{\partial S_{\ell s}}{\partial p}\right)_j\right)\Bigg]$$

$$=P_j^n\Bigg[-\left((\rho_\ell\alpha)_j^r\left(\frac{\partial\rho_g}{\partial p}\right)_j+(\rho_g\alpha^\ell)_j^r\left(\frac{\partial\rho_\ell}{\partial p}\right)_j\right)$$

$$-\frac{(\rho_\ell-\rho_g)_j^r\,(T_s)_j^r}{(h_{gs}-h_{\ell s})_j^r}\left((F_{gs})_j^{n+1}(\alpha\rho_g)_j^r\left(\frac{\partial S_{gs}}{\partial p}\right)_j+(F_{\ell s})_j^{n+1}(\alpha^\ell\rho_\ell)_j^r\left(\frac{\partial S_{\ell s}}{\partial p}\right)_j\right)\Bigg]-\Delta t(\rho_\ell-\rho_g)_j^r\,\dot{m}_{\Delta T}$$

$$+\left(\frac{\Delta t}{\Delta x}\right)(\rho_\ell)_j^r\left[(\alpha\rho_g v^g)_{j+\frac{1}{2}}^n-(\alpha\rho_g v^g)_{j-\frac{1}{2}}^n\right]+\left(\frac{\Delta t}{\Delta x}\right)(\rho_g)_j^r\left[(\alpha^\ell\rho_\ell v^\ell)_{j+\frac{1}{2}}^n-(\alpha^\ell\rho_\ell v^\ell)_{j-\frac{1}{2}}^n\right]$$

$$-\left(\frac{\Delta t}{\Delta x}\right)^2(\rho_\ell)_j^r\left[(\alpha\rho_g v^g v^g)_{j+1}^r-2\,(\alpha\rho_g v^g v^g)_j^r+(\alpha\rho_g v^g v^g)_{j-1}^r\right]$$

$$-\left(\frac{\Delta t}{\Delta x}\right)^2(\rho_g)_j^r\left[(\alpha^\ell\rho_\ell v^\ell v^\ell)_{j+1}^r-2\,(\alpha^\ell\rho_\ell v^\ell v^\ell)_j^r+(\alpha^\ell\rho_\ell v^\ell v^\ell)_{j-1}^r\right]$$

$$-\frac{\Delta t^2}{\Delta x}(\rho_\ell)_j^r\left((\bar{A}_{wg}B_{wg}v^g)_{j+\frac{1}{2}}^r-(\bar{A}_{wg}B_{wg}v^g)_{j-\frac{1}{2}}^r\right)-\frac{\Delta t^2}{\Delta x}(\rho_g)_j^r\left((\bar{A}_{w\ell}B_{w\ell}v^\ell)_{j+\frac{1}{2}}^r-(\bar{A}_{w\ell}B_{w\ell}v^\ell)_{j-\frac{1}{2}}^r\right)$$

$$+\frac{\Delta t^2}{\Delta x}(\rho_\ell-\rho_g)_j^r\left[\left((\dot{m}\hat{v})_{j+\frac{1}{2}}^r-(\dot{m}\hat{v})_{j-\frac{1}{2}}^r\right)-\left((\bar{A}_{g\ell}B_{g\ell}(v^g-v^\ell))_{j+\frac{1}{2}}^r-(A_{g\ell}B_{g\ell}(v^g-v^\ell))_{j-\frac{1}{2}}^r\right)\right]$$

$$+\frac{\Delta t^2}{\Delta x}g_x(\rho_\ell)_j^r\left((\alpha\rho_g)_{j+\frac{1}{2}}^r-(\alpha\rho_g)_{j-\frac{1}{2}}^r\right)+\frac{\Delta t^2}{\Delta x}g_x(\rho_g)_j^r\left((\alpha^\ell\rho_\ell)_{j+\frac{1}{2}}^r-(\alpha^\ell\rho_\ell)_{j-\frac{1}{2}}^r\right)$$

$$+(\rho_\ell\alpha)_j^r\left(\frac{\partial\rho_g}{\partial u_g}\right)_j^n\left((u_g)_j^{n+1}-(u_g)_j^n\right)+(\rho_g\alpha^\ell)_j^r\left(\frac{\partial\rho_\ell}{\partial u_\ell}\right)_j^n\left((u_\ell)_j^{n+1}-(u_\ell)_j^n\right). \tag{33}$$

The iteration cycle begins with the solution of the pressure equation. The other iteration equations are given in the order in which they are solved.

State Equation

$$(\rho_g)_j^{r+1} = \rho_g\,(p_j^{r+1},\ (u_g)_j^{n+1}) \tag{34}$$

and

$$(\rho_\ell)_j^{r+1} = \rho_\ell\,(p_j^{r+1},\ (u_\ell)_j^{n+1})\ . \tag{35}$$

Vapor Momentum Equation

$$\frac{(\alpha)^r_{j+\frac{1}{2}}\,(\rho_g)^{r+1}_{j+\frac{1}{2}}\,(v^g)^{r+1}_{j+\frac{1}{2}} - (\alpha\rho_g v^g)^n_{j+\frac{1}{2}}}{\Delta t} + \frac{1}{\Delta x}\left[(\alpha v^g)^r_{j+\frac{1}{2}}\,(\rho_g)^{r+1}_{j+\frac{1}{2}}\,(v^g)^{r+1}_{j+1}\right.$$

$$\left. - (\alpha v^g)^r_{j-\frac{1}{2}}\,(\rho_g)^{r+1}_{j-\frac{1}{2}}\,(v^g)^{r+1}_{j-1}\right] = -\,\alpha^r_{j+\frac{1}{2}}\,\frac{p^{r+1}_{j+1} - p^{r+1}_j}{\Delta x}$$

$$+\,\dot{m}^r_{j+\frac{1}{2}}\,\hat{v}^r_{j+\frac{1}{2}} - (\bar{\Lambda}_{g\ell}B_{g\ell})^r_{j+\frac{1}{2}}\left((v^g)^{r+1}_{j+\frac{1}{2}} - (v^\ell)^r_{j+\frac{1}{2}}\right)$$

$$-\,(\bar{\Lambda}_{wg}B_{wg})^r_{j+\frac{1}{2}}\,(v^g)^{r+1}_{j+\frac{1}{2}} + \alpha^r_{j+\frac{1}{2}}\,(\rho_g)^{r+1}_{j+\frac{1}{2}}\,g_x\ . \tag{36}$$

Liquid Momentum Equation

$$\frac{(\alpha^{\ell})^{r}_{j+\frac{1}{2}} (\rho_{\ell})^{r+1}_{j+\frac{1}{2}} (v^{\ell})^{r+1}_{j+\frac{1}{2}} - (\alpha^{\ell}\rho_{\ell}v^{\ell})^{n}_{j+\frac{1}{2}}}{\Delta t} + \frac{1}{\Delta x}\left[(\alpha^{\ell}v^{\ell})^{r}_{j+\frac{1}{2}} (\rho_{\ell})^{r+1}_{j+\frac{1}{2}} (v^{\ell})^{r+1}_{j+1}\right.$$

$$\left. - (\alpha^{\ell}v^{\ell})^{r}_{j-\frac{1}{2}} (\rho_{\ell})^{r+1}_{j-\frac{1}{2}} (v^{\ell})^{r+1}_{j-1}\right] = - (\alpha^{\ell})^{r}_{j+\frac{1}{2}} \frac{P^{r+1}_{j+1} - P^{r+1}_{j}}{\Delta x}$$

$$- \dot{m}^{r}_{j+\frac{1}{2}} \hat{v}^{r}_{j+\frac{1}{2}} - (\bar{A}_{g\ell}B_{g\ell})^{n}_{j+\frac{1}{2}} \left((v^{\ell})^{r+1}_{j+\frac{1}{2}} - (v^{g})^{r}_{j+\frac{1}{2}}\right)$$

$$- (\bar{A}_{w\ell}B_{w\ell})^{r}_{j+\frac{1}{2}} (v^{\ell})^{r+1}_{j+\frac{1}{2}} + (\alpha^{\ell})^{r}_{j+\frac{1}{2}} (\rho_{\ell})^{r+1}_{j+\frac{1}{2}} g_{x} \quad . \tag{37}$$

Liquid Continuity Equation

$$\frac{(\alpha^{\ell}\rho_{\ell})^{r+1}_{j} - (\alpha^{\ell}\rho_{\ell})^{n}_{j}}{\Delta t} + \frac{(\alpha^{\ell}\rho_{\ell}v^{\ell})^{r+1}_{j+\frac{1}{2}} - (\alpha^{\ell}\rho_{\ell}v^{\ell})^{r+1}_{j-\frac{1}{2}}}{\Delta x} = - \dot{m}^{r+1}_{j} \quad . \tag{38}$$

A flowchart showing the steps of the iteration is shown in Figure 1. Numerical experiments have shown that other arrangements of the discrete field equations are possible without affecting the convergence of the numerical technique.

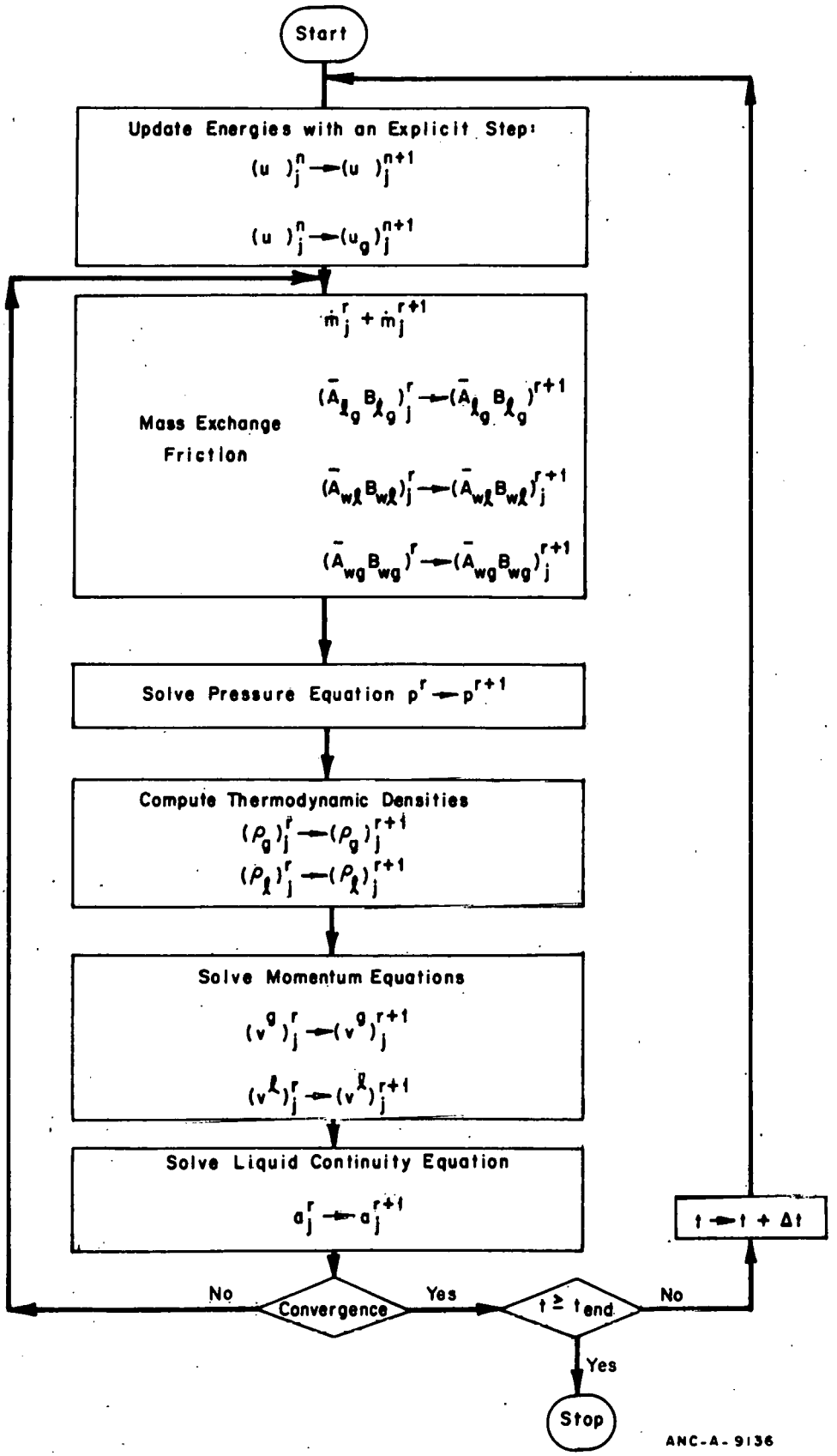

Fig. 1 UVUT SCIMP scheme flow.

2. THE ICE-PF METHOD

The ICE-PF method is characterized by the simultaneous solution of the finite differenced continuity equations, Equations (10a), and (11a), for the pressure and void fraction in each computational cell.

Let

$$C^g = (\alpha\rho_g)_j^{n+1} - (\alpha\rho_g)_j^n + \frac{\Delta t}{\Delta x}\left[\langle\alpha\rho_g v^g\rangle_{j+\frac{1}{2}}^{n+1} - \langle\alpha\rho_g v^g\rangle_{j-\frac{1}{2}}^{n+1}\right] - \dot{m}_j^{n+1}\,\Delta t \tag{39}$$

and

$$C^\ell = (\alpha^\ell\rho_\ell)_j^{n+1} - (\alpha^\ell\rho_\ell)_j^n + \frac{\Delta t}{\Delta x}\left[\langle\alpha^\ell\rho_\ell v^\ell\rangle_{j+\frac{1}{2}}^{n+1} - \langle\alpha^\ell\rho_\ell v^\ell\rangle_{j-\frac{1}{2}}^{n+1}\right] + \dot{m}_j^{n+1}\,\Delta t. \tag{40}$$

The corner brackets used in Equations (39) and (40) represent either centered differences or donor cell differences[a] as is appropriate for the particular problem being solved.

Assuming that $C^\ell = C^\ell(P,\alpha)$ and $C^g = C^g(P,\alpha)$, the nonlinear system

$$\begin{aligned} C^g &= 0 \\ C^\ell &= 0 \end{aligned} \tag{41}$$

is solved simultaneously for P and α using a modification of Newton's method.

For the System (41) Newton's method can be written as

$$\begin{bmatrix} \frac{\partial C^g}{\partial P_j^r} & \frac{\partial C^g}{\partial \alpha_j^r} \\ \frac{\partial C^\ell}{\partial P_j^r} & \frac{\partial C^\ell}{\partial \alpha_j^r} \end{bmatrix} \begin{bmatrix} \Delta P_j^{r+1} \\ \Delta \alpha_j^{r+1} \end{bmatrix} = \begin{bmatrix} -C^{gr} \\ -C^{\ell r} \end{bmatrix} \tag{42}$$

[a] The donor cell flux $\langle Qv\rangle_{j+\frac{1}{2}}$ of a quanity Q is defined by

$$\langle Qv\rangle_{j+\frac{1}{2}} = \begin{cases} Q_j v_{j+\frac{1}{2}} & \text{if } v_{j+\frac{1}{2}} \geq 0 \\ Q_{j+1} v_{j+\frac{1}{2}} & \text{if } v_{j+\frac{1}{2}} < 0. \end{cases}$$

The superscripts r and r+1 indicate old and new iterates at time $(n+1)\Delta t$ and

$$\Delta P_j^{r+1} \equiv P_j^{r+1} - P_j^r$$

$$\Delta \alpha_j^{r+1} \equiv \alpha_j^{r+1} - \alpha_j^r \,. \tag{43}$$

The centered difference continuity equations, Equations (10) and (11), are used to obtain approximations to the derivatives in the Jacobian matrix of Equation (42). For example

$$\frac{\partial C^g}{\partial P_j^r} \approx \frac{\alpha_j^r}{\Delta t}\left(\frac{\partial \rho_g}{\partial P}\right)_j^r + \frac{(\alpha\rho_g)^r_{j+\frac{1}{2}}}{\Delta x}\frac{\partial (v^g)^r_{j+\frac{1}{2}}}{\partial P_j^r} + \frac{1}{2}\frac{(\alpha v^g)^r_{j+\frac{1}{2}}}{\Delta x}\left(\frac{\partial \rho_g}{\partial P}\right)_j^r$$

$$- \frac{(\alpha\rho_g)^r_{j-\frac{1}{2}}}{\Delta x}\frac{\partial (v^g)^r_{j-\frac{1}{2}}}{\partial P_j^r} - \frac{1}{2}\frac{(\alpha v^g)^r_{j-\frac{1}{2}}}{\Delta x}\left(\frac{\partial \rho_g}{\partial P}\right)_j^r - \frac{\partial \dot{m}_j^r}{\partial P_j^r} \tag{44}$$

and

$$\frac{\partial C^g}{\partial \alpha_j^r} \approx \frac{(\rho_g)_j^r}{\Delta t} + \frac{(\rho_g v^g)^r_{j+\frac{1}{2}}}{2\Delta x} - \frac{(\rho_g v^g)^r_{j-\frac{1}{2}}}{2\Delta x} - \left(\frac{\partial \dot{m}}{\partial \alpha}\right)_j^r . \tag{45}$$

Similar expressions are obtained for $\frac{\partial C^\ell}{\partial P_j^r}$ and $\frac{\partial C^\ell}{\partial \alpha_j^r}$ using Equation (11).

The Expressions (44) and (45) are not yet in a form suitable for computation since the partial derivatives

$\frac{\partial (vg)^r_{j+\frac{1}{2}}}{\partial P_j^r}$, $\frac{\partial (vg)^r_{j-\frac{1}{2}}}{\partial P_j^r}$, $\left(\frac{\partial \dot{m}}{\partial P}\right)_j^r$, and $\left(\frac{\partial \dot{m}}{\partial \alpha}\right)_j^r$ are required.

In addition, the expressions for $\frac{\partial C^\ell}{\partial P_j^r}$ and $\frac{\partial C^\ell}{\partial \alpha_j^r}$ will include $\frac{\partial (v^\ell)^r_{j+\frac{1}{2}}}{\partial P_j^r}$ and $\frac{\partial (v^\ell)^r_{j-\frac{1}{2}}}{\partial P_j^r}$.

Expressions approximating these derivatives are obtained using the finite differenced momentum equations, Equations (12a) and (13a), and the constitutive flashing rate equation, Equation (32).

The finite differenced nonconservative momentum equations, Equations (12a) and (13a), are linear in the velocities $(v^g)^{n+1}_{j+\frac{1}{2}}$ and $(v^\ell)^{n+1}_{j+\frac{1}{2}}$ and may be written

$$V_1(v^g)^{n+1}_{j+\frac{1}{2}} + V_2(v^\ell)^{n+1}_{j+\frac{1}{2}} = V_3$$

and

$$L_1(v^g)^{n+1}_{j+\frac{1}{2}} + L_2(v^\ell)^{n+1}_{j+\frac{1}{2}} = L_3. \tag{46}$$

When, for example, $\dot{m}^{n+1}_{j+\frac{1}{2}} > 0$ and the intrinsic velocity $\hat{v}^{n+1}_{j+\frac{1}{2}}$ is taken to be $(v^\ell)^{n+1}_{j+\frac{1}{2}}$, the coefficients, V_1 and L_1, are

$$V_1 = \frac{(\alpha^g \rho_g)^n_{j+\frac{1}{2}}}{\Delta t} + \dot{m}^{n+1}_{j+\frac{1}{2}} + \bar{A}_{g\ell}B_{g\ell} + \bar{A}_{wg}B_{wg}$$

and

$$L_1 = -\bar{A}_{g\ell}B_{g\ell}.$$

When $\dot{m}^{n+1}_{j+\frac{1}{2}} < 0$ and the intrinsic velocity $v^{n+1}_{j+\frac{1}{2}}$ is taken to be $(v^g)^{n+1}_{j+\frac{1}{2}}$, these coefficients are

$$V_1 = \frac{(\alpha^g \rho_g)^n_{j+\frac{1}{2}}}{\Delta t} + \bar{A}_{g\ell}B_{g\ell} + \bar{A}_{wg}B_{wg}$$

and

$$L_1 = \dot{m}^{n+1}_{j+\frac{1}{2}} - \bar{A}_{g\ell}B_{g\ell} \quad \text{respectively.}$$

Similarily expressions may be obtained by inspection from Equations (12a) and (13a) for V_2, V_3, L_2, and L_3 for the cases $\dot{m}^{n+1}_{j+\frac{1}{2}} > 0$ and $\dot{m}^{n+1}_{j+\frac{1}{2}} < 0$.

Solution of the linear System (46) produces

$$(v^g)^{n+1}_{j+\frac{1}{2}} = \frac{1}{DETM}[L_2V_3 - V_2L_3] \tag{47}$$

and

$$(v^\ell)^{n+1}_{j+\frac{1}{2}} = \frac{1}{DETM}[-L_1V_3 + V_1L_3]. \tag{48}$$

DETM = $V_1 L_2 - L_1 V_2$ is the determinant of the system. Then the momentum equations are differenced about the point $(j-\frac{1}{2})\Delta x$ and the resulting equations solved simultaneously for $(vg)^{n+1}_{j-\frac{1}{2}}$ and $(v^{\ell})^{n+1}_{j-\frac{1}{2}}$. Now the expressions for

$$\frac{\partial (vg)^{n+1}_{j+\frac{1}{2}}}{\partial P^{n+1}_j}, \quad \frac{\partial (v^{\ell})^{n+1}_{j+\frac{1}{2}}}{\partial P^{n+1}_j}, \quad \frac{\partial (vg)^{n+1}_{j-\frac{1}{2}}}{\partial P^{n+1}_j}, \text{ and } \quad \frac{\partial (v^{\ell})^{n+1}_{j-\frac{1}{2}}}{\partial P^{n+1}_j}$$

are obtained by formal differentiation of Equation (47), Equation (48), and the analogous equations for $(vg)^{n+1}_{j-\frac{1}{2}}$ and $(v^{\ell})^{n+1}_{j-\frac{1}{2}}$.

In order to obtain approximations to $\dfrac{\partial \dot{m}^{n+1}_j}{\partial P^{n+1}_j}$ and $\dfrac{\partial \dot{m}^{n+1}_j}{\partial \alpha^{n+1}_j}$ a finite difference form of Equation (32) is differentiated and the following expressions are used in the approximate Jacobian matrix

$$\frac{\partial \dot{m}^{n+1}_j}{\partial P^{n+1}_j} \approx \frac{-\Gamma^{n+1}_{s_j}}{h^{n+1}_{gs_j} - h^{n+1}_{\ell s_j}} \left[F_{gs} \alpha \rho_g \frac{\partial S_{gs}}{\partial P} + F_{\ell s} \alpha^{\ell} \rho_{\ell} \frac{\partial S_{\ell s}}{\partial P} \right]^{n+1}_j \frac{1}{\Delta t} \tag{49}$$

$$\frac{\partial \dot{m}^{n+1}_j}{\partial \alpha^{n+1}_j} \approx \frac{-\Gamma^{n+1}_{s_j}}{h^{n+1}_{gs_j} - h^{n+1}_{\ell s_j}} \left[F_{gs} \rho_g \frac{\partial S_{gs}}{\partial P} - F_{\ell} \rho_{\ell} \frac{\partial S_{\ell s}}{\partial P} \right]^{n+1}_j \frac{P^{n+1}_j - P^n_j}{\Delta t}. \tag{50}$$

The dependent variables for a UVUT problem are determined by solving:

(1) The energy equations, Equations (14) and (15), for u_{ℓ} and u_s

(2) The continuity equations, Equations (39) and (40), for P and α

(3) The momentum equations, Equations (12a) and (13a), for vg and v^{ℓ}

(4) The state equations for the thermodynamic densities, ρ_g and ρ_{ℓ}.

The explicit energy equations are solved first, followed by an explicit update of the momentum equations. The pressure and void fraction are then determined iteratively by

solving the system [Equation (41)] as described above. The velocities are readjusted during the iteration cycle to account for the changes in pressure using

$$(v^{\ell})^{r+1}_{j+\frac{1}{2}} = (v^{\ell})^{r}_{j+\frac{1}{2}} + \frac{\partial (v^{\ell})^{r}_{j+\frac{1}{2}}}{\partial p^{r}_{j}} (p^{r+1}_{j} - p^{r}_{j}) \tag{51}$$

and

$$(v^{g})^{r+1}_{j+\frac{1}{2}} = (v^{g})^{r}_{j+\frac{1}{2}} + \frac{\partial (v^{g})_{j+\frac{1}{2}}}{\partial p^{r}_{j}} (p^{r+1}_{j} - p^{r}_{j}). \tag{52}$$

Also the thermodynamic densities are updated during the iterative cycle using Equations (34) and (35). A flowchart showing the flow of the ICE-PF method is given in Figure 2.

The ICE-PF method is a "cell-by-cell" iteration. That is, the full set of iteration equations are solved in a mesh cell before moving to the next cell. This is contrasted with the SCIMP method in which an equation is solved on the whole finite difference mesh before solving the next equation.

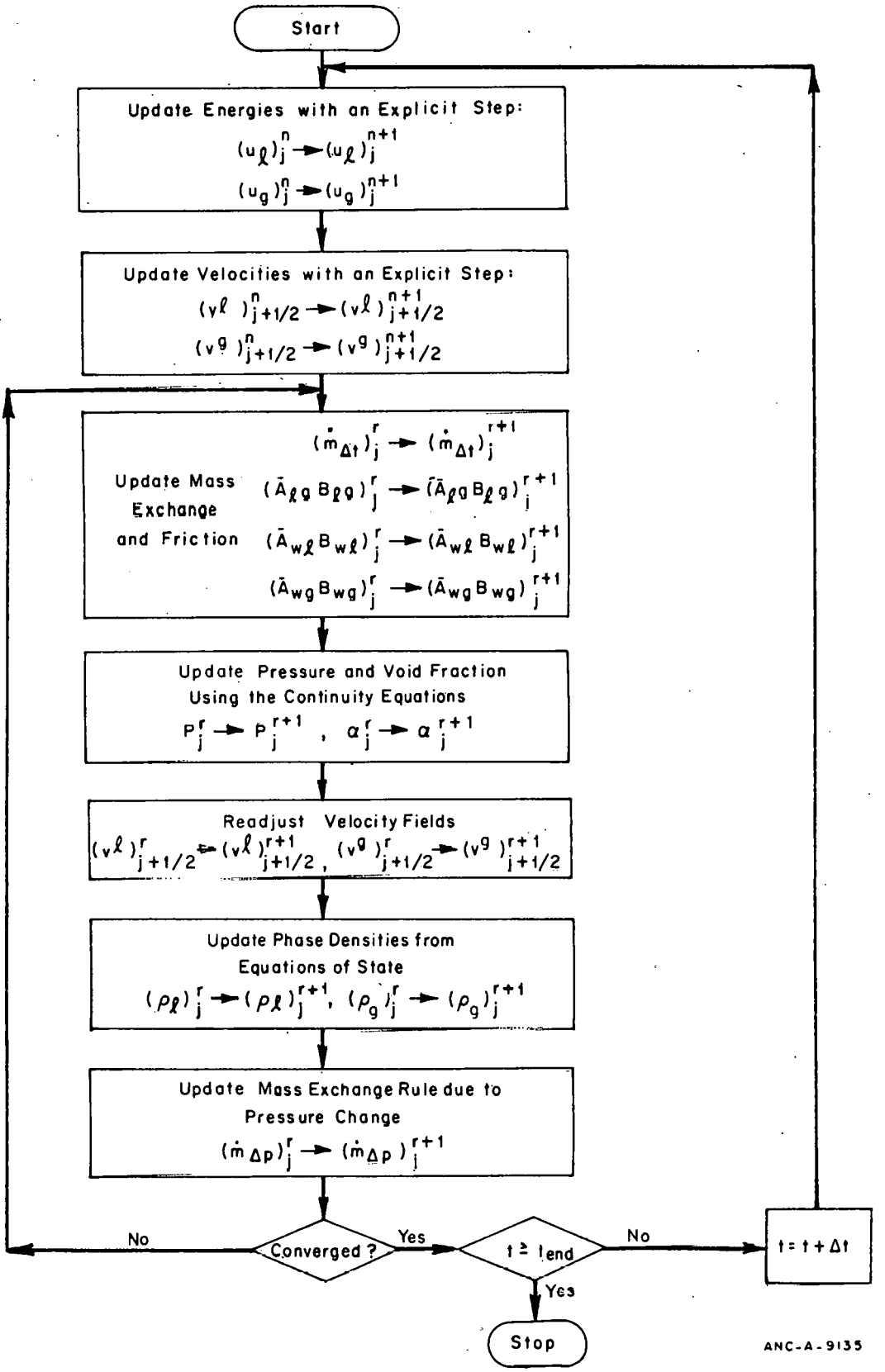

Fig. 2 UVUT ICE-PF scheme flow.

V. COMPUTATIONAL RESULTS

This section documents a comparison of STUBE code calculations with data from a pipe depressurization experiment by Edwards and O'Brien[9]. In this experiment a straight pipe 13.44 feet long with an inside diameter of 2.88 inches was filled with subcooled water initially pressurized to 1,014.7 psia at a temperature of 465°F. The experiment was conducted by breaking a diaphram at one end of the pipe so that the fluid emptied into the surroundings. Data were taken at locations designated as GS-1 through GS-7, with GS-1 near the break and GS-7 near the closed end of the pipe. The location of the measuring devices of interest are shown on the plots comparing experimental data and the calculated results (Figures 3 through 11).

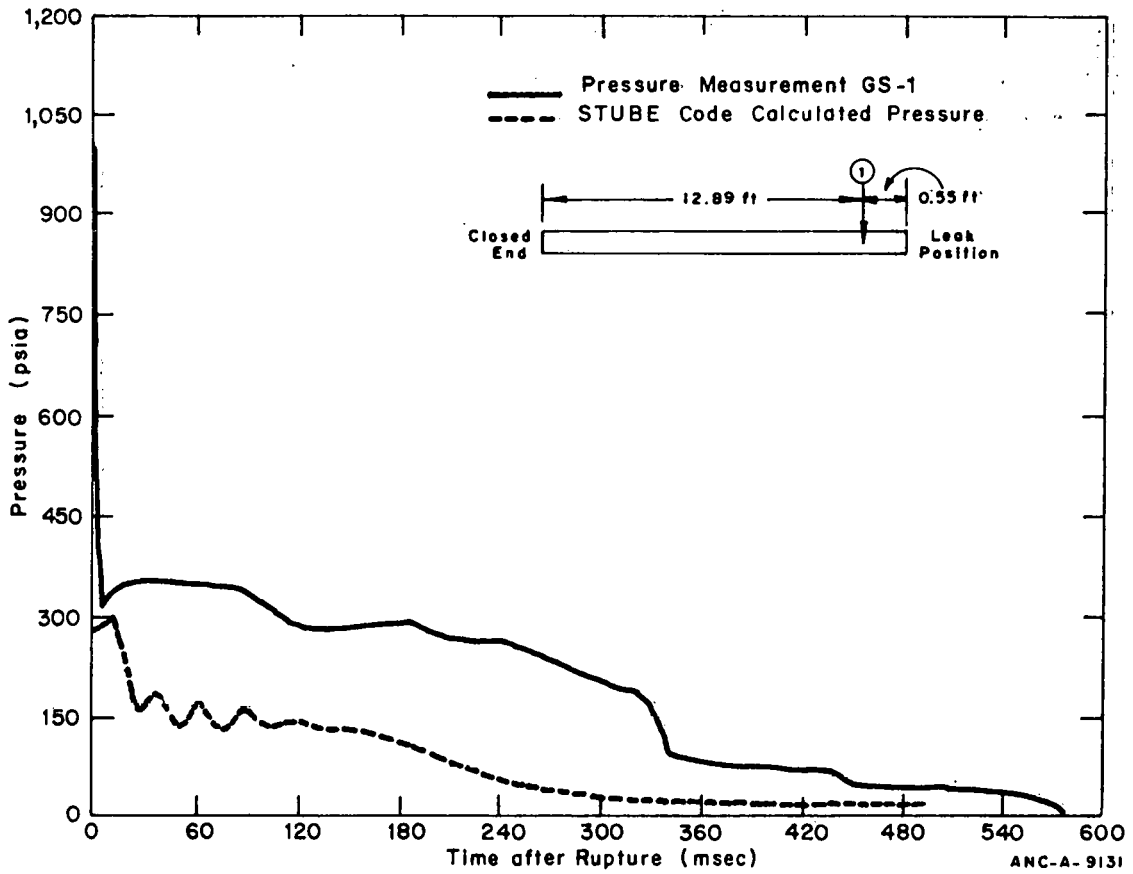

Fig. 3 Long-term comparison between measurement and STUBE code calculation of pressure at GS-1 in Edwards' experiment.

The pipe depressurization experiment was modeled for the STUBE code by nine equal size computational cells, with uniform initial pressure and enthalpy distributions along the length of the pipe. The flow regime during the transient was determined by Baker's flow regime map, and consistent friction correlations were used to compute interphase and wall frictions. All correlations used by STUBE to obtain the results presented in this document are taken from Solbrig et al[8].

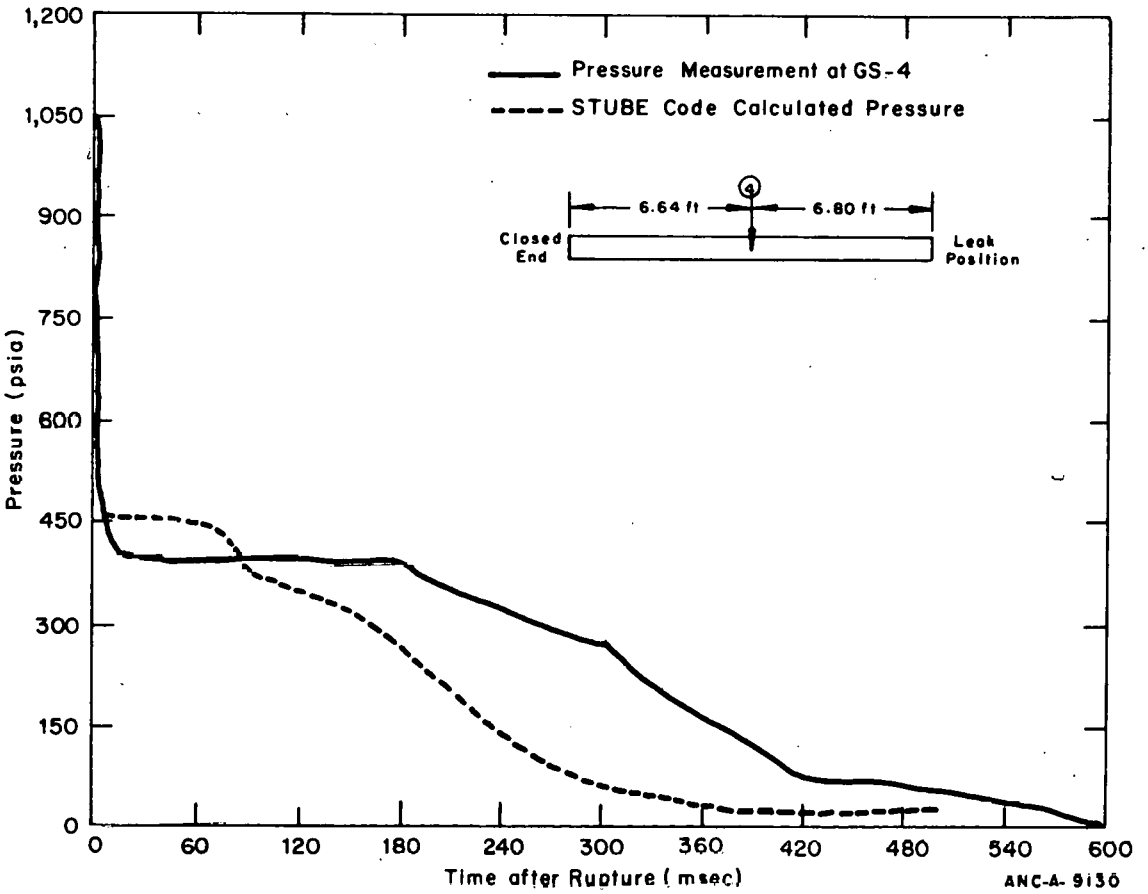

Fig. 4 Long-term comparison between measurement and STUBE code calculation of pressure at GS-4 in Edwards' experiment.

The internal energy of each phase was computed, using the appropriate energy equation when there was no mass exchange between the phases. When there was mass exchange between the phases, the internal energies of the liquid and vapor phases were taken to be saturation values at the local pressure (UVET flow).

The pressure at the outlet boundary was calculated by averaging the pressure in the first cell upstream of the break and the ambient pressure. The outlet boundary was modeled using the full flow area and no loss coefficients.

Shown in Figures 3 through 11 are comparisons of experimental data and STUBE code calculations. Figures 3 through 8 illustrate long-term comparisons with a time scale of 0-600 msec. Figures 9 through 11 illustrate short-term comparisons with a time scale of 0-15 msec.

In Figures 3 through 5, calculated pressures are compared with data at the open end, center, and closed end of the pipe. Figure 3 shows that the outlet pressure as presently computed underestimates the experimental data by a considerable amount, indicating a more refined model is needed for the outlet pressure boundary condition.

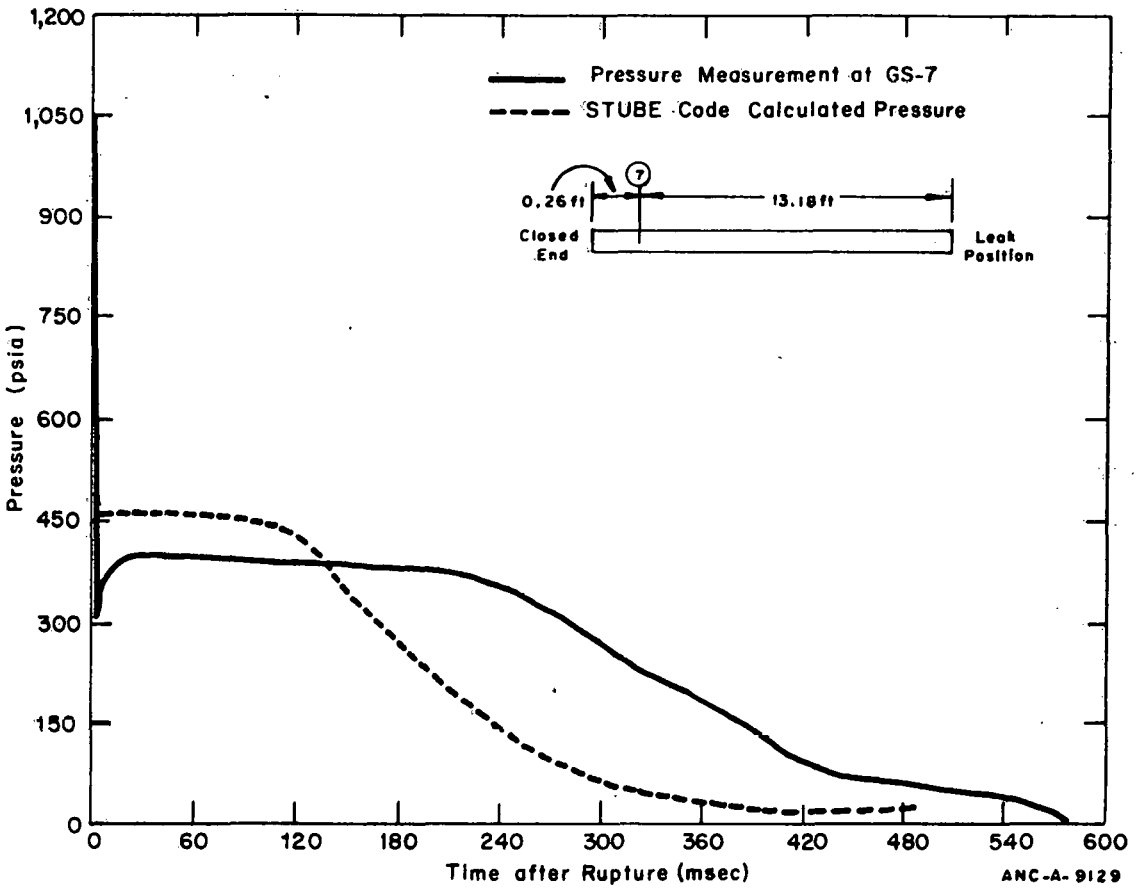

Fig. 5 Long-term comparison between measurement and STUBE code calculation of pressure at GS-7 in Edwards' experiment.

In Figure 4 the STUBE code results and the experimental data are shown at the center of the tube (GS-4). The pressure is overpredicted up to 60 msec. This could be due to the model used for phase change due to pressure change or to the initial enthalpy distribution. Past 60 msec, a low pressure is calculated by the STUBE code for the long-term transient. This result is typical of many fluid dynamic codes and could be caused by the outlet boundary condition.

Figure 6 shows a comparison of long-term transient void fraction at GS-5. Figure 6 illustrates a reasonable agreement between the STUBE code calculation of void fraction and the experiment.

The results of the calculated phase velocities at the outlet are shown in Figure 7. No experimental data were obtained in the experiment for the phase velocities and, consequently, no comparisons can be made. The gas phase velocity is much higher than the liquid because of the lower mass of the vapor. The oscillations which appear in the velocities between 10 and 100 msec are correlated well with changes in the flow regime. The Baker model predicts that the flow starts in separated flow, switches back and forth between

separated and annular flow, and eventually remains in annular flow until near the end of the transient, when the regime reverts back to separated flow. These oscillations evidence the need for smoother transitions between regimes.

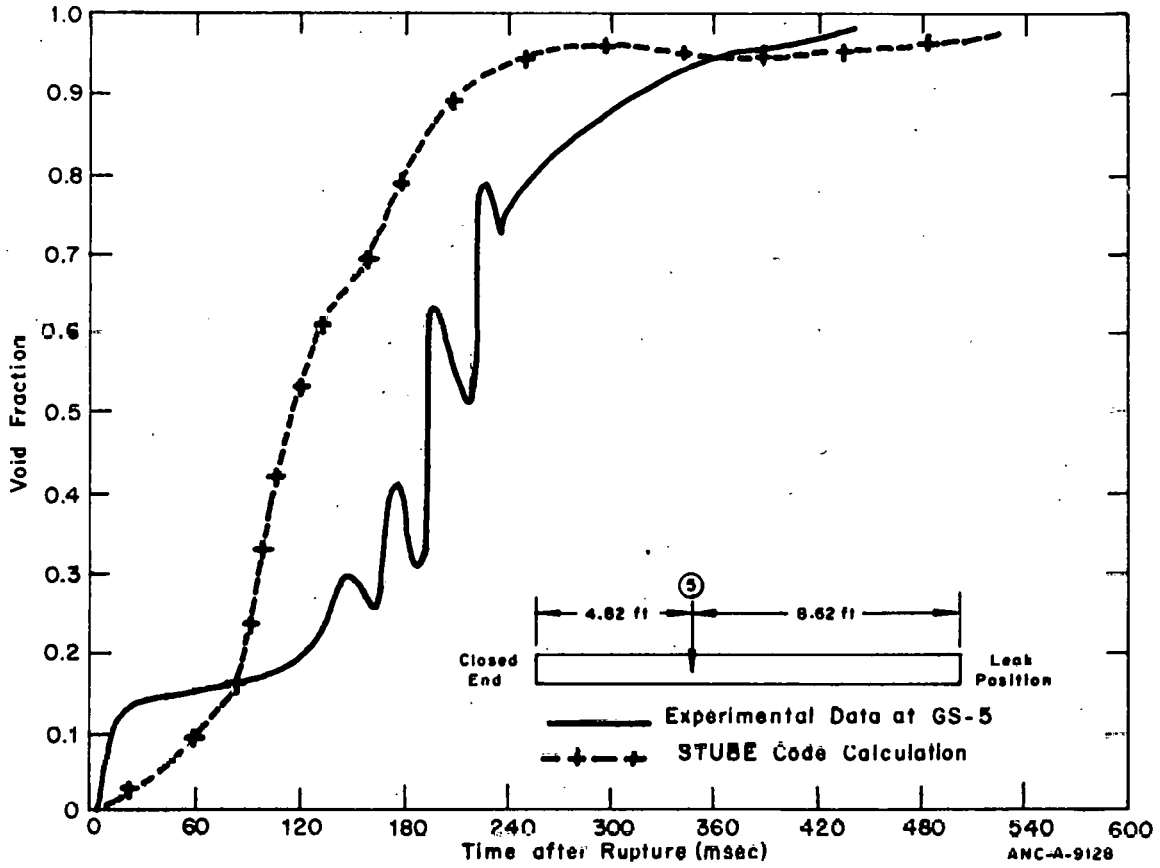

Fig. 6 Comparison of experiment and STUBE code calculation of void fraction at GS-5.

A plot of the liquid and vapor velocities at the center of the pipe is given in Figure 8. During most of the transient, the vapor velocity is higher than the liquid velocity. A maximum slip ratio near 10 is reached at about 380 msec. This value is in close agreement with the value computed from the theory of Levy[10]. At approximately 400 msec, the pressure inside the pipe drops below ambient, and the vapor flow reverses directions throughout the pipe. The liquid velocity does not become negative, but the average velocity of the liquid and vapor does. The negative flow increases the pressure above ambient, and the vapor velocity becomes positive again. No STUBE runs were made beyond 500 msec to check whether the vapor velocity oscillations damp to eventually reach a steady state.

Figures 9 through 11 show short-term (0 to 15 msec) pressure comparisons. The outlet pressure undershoot shown in Figure 9 is caused by the break boundary condition which has been discussed previously. At the center of the pipe (GS-4) the STUBE code calculates pressures higher than experimentally measured (Figure 10). The pressure

calculated at the closed end, (GS-7) shown in Figure 11, is higher than experimental. The pressure dip at 4 msec was not predicted with the STUBE code, because it uses a mass transfer model which assumes equilibrium thermodynamics. An example of the pressure prediction using nonequilibrium thermodynamics in the mass transfer model can be found in Rivard and Torry[11].

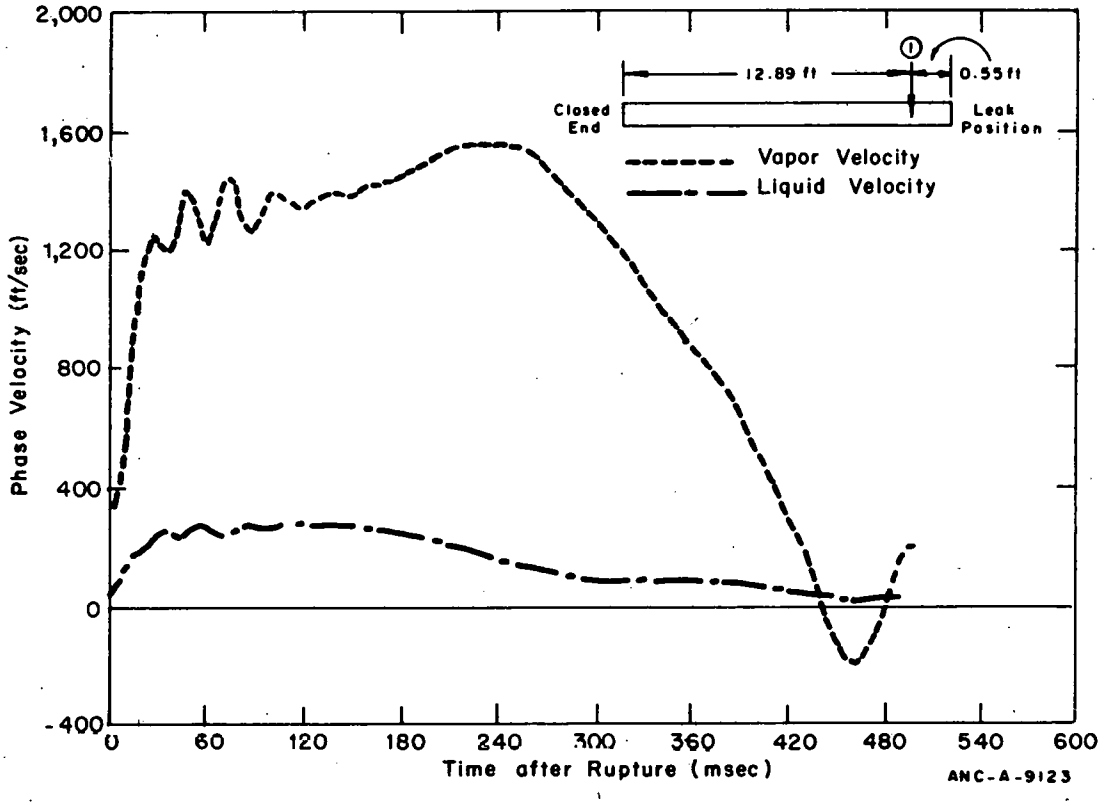

Fig. 7 Comparison of vapor and liquid velocities at GS-1 in Edwards' experiment.

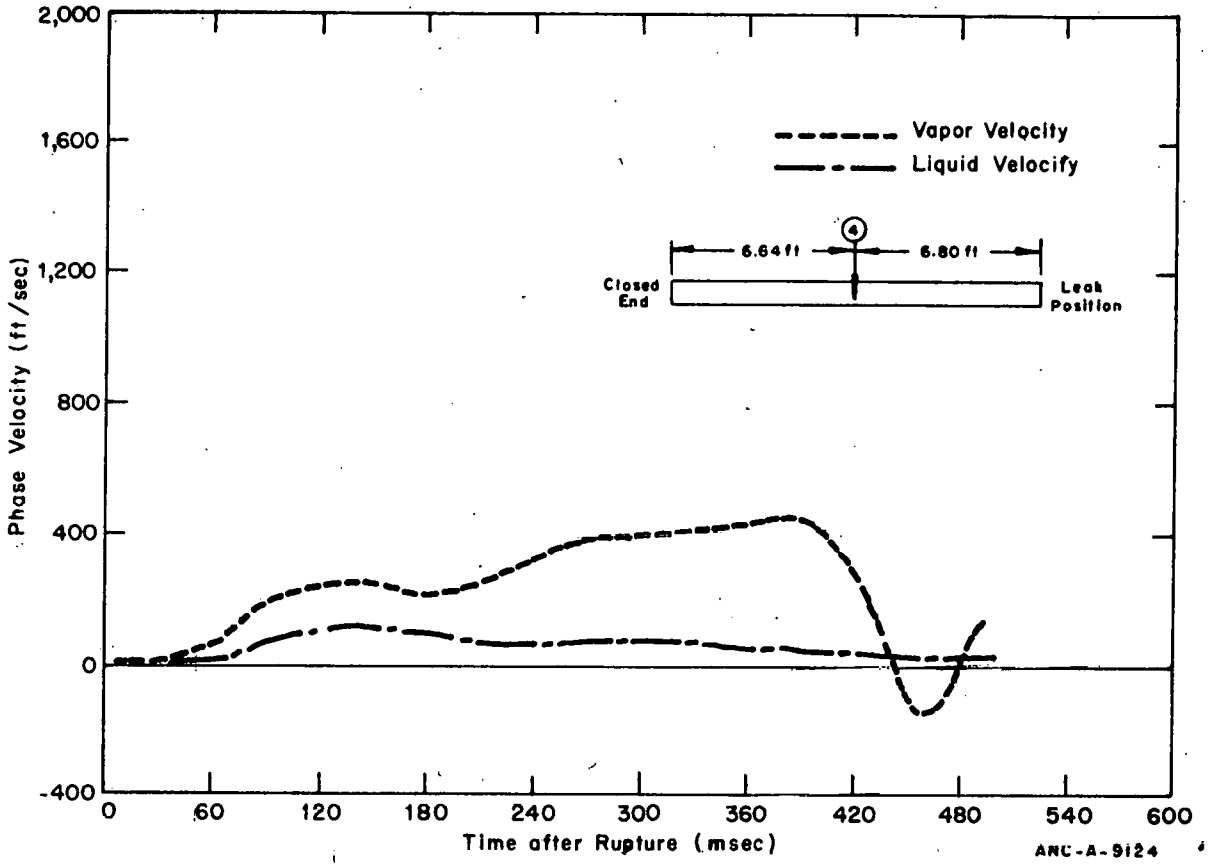

Fig. 8 Comparison of vapor and liquid velocities at GS-4 in Edwards' experiment.

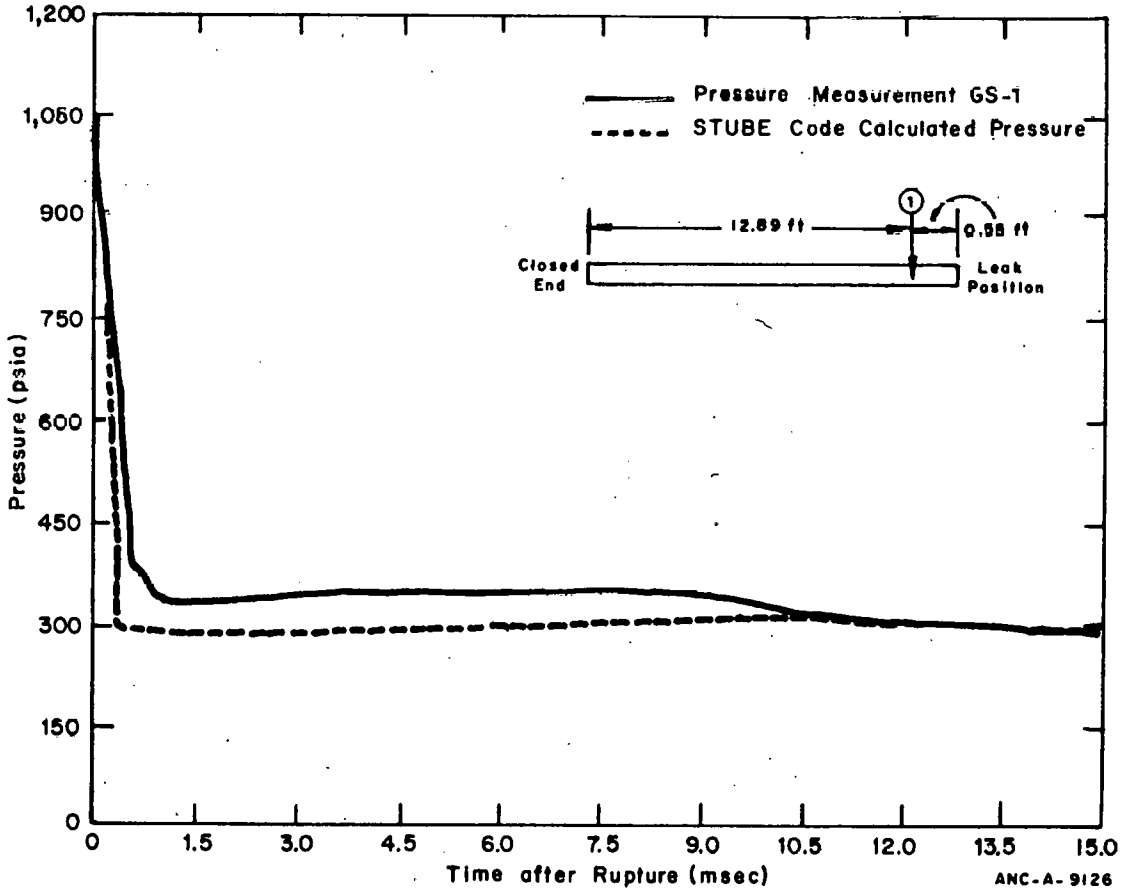

Fig. 9 Short-term comparison between measurement and STUBE code calculation of pressure at GS-1 in Edwards' experiment.

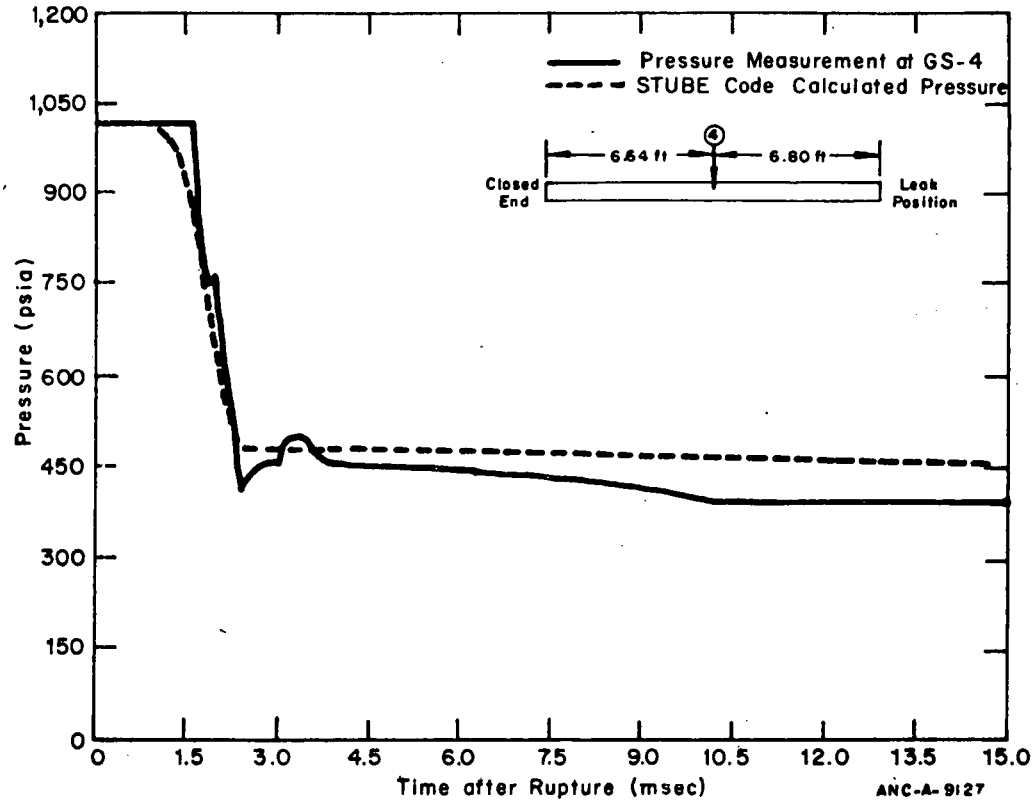

Fig. 10 Short-term comparison between measurement and STUBE code calculation of pressure at GS-4 in Edwards' experiment.

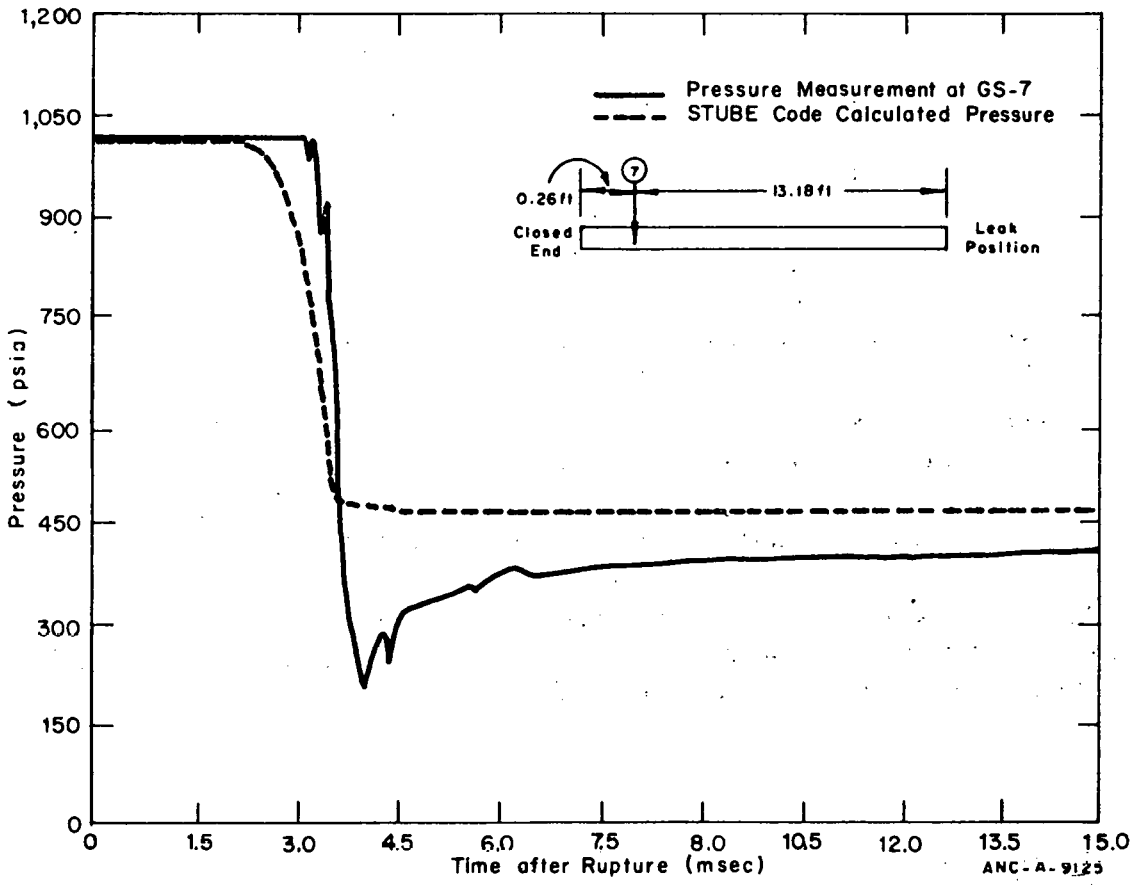

Fig. 11 Short-term comparison between measurement and STUBE code calculation of pressure at GS-7 in Edwards' experiment.

VI. CONCLUSIONS

Finite difference equations have been derived which numerically model the governing equations for a seriated continuum. The difference equations are the basis for two numerical schemes which are used to compute both unequal phase velocities and unequal phase temperatures in transient two-phase flows. The difference equations are highly implicit, allowing application to all flow speeds. A disadvantage to an implicit formulation is the requirement of solving a tightly coupled system of nonlinear equations.

In Section IV the SCIMP and ICE-PF methods for solving the finite difference equations are described. The ICE-PF method allows the solution to proceed on a cell-by-cell basis, whereas SCIMP solves each equation on the entire finite difference mesh. The SCIMP method can also be recast as a cell-by-cell method in a straightforward manner. Preliminary computations with a cell-by-cell version also gave satisfactory results. The SCIMP method is formulated with the momentum flux terms at the advanced time level; the ICE-PF method has them at old time. Preliminary investigations indicate that a satisfactory version of ICE-PF with implicit momentum flux can be formulated.

Although the SCIMP pressure predictions presented in Section V compare favorably with results from homogeneous flow models, the lack of agreement between the computational results and the experimental data indicates that further work is required on the constitutive models employed in the STUBE code. Needed improvements presently identified include:

(1) Outlet boundary conditions

(2) Smoothing the friction terms during flow regime transitions

(3) Constitutive equations for the slug flow regime

(4) A method of applying steady state flow regime maps to transient flows, especially for low-flow cases

(5) Constitutive equations for interphase mass and energy exchange.

Additional work is also required on the energy equations. With the energy equations outside the iteration loop, further investigation is required to determine how these affect the mass and energy exchange associated with changes in pressure, which are computed inside the iteration loop.

The computational results presented in Section V and other unpublished results from the STUBE code indicate that the basic numerical models presented are capable of

computing unequal velocities and unequal temperatures in two-phase flows. The numerical schemes could be used as the basis for a complete UVUT OR UVET reactor systems code.

VII. REFERENCES

1. F. H. Harlow and A. A. Amsden, "Numerical Calculation of Multiphase Fluid Flow," *Journal of Computational Physics, 17* (1975) pp 19-52.

2. R. W. Lyczkowski et al, *Characteristics and Stability Analyses of Transient One-Dimensional Two-Phase Flow Equations and Their Finite Difference Approximations,* ASME Paper 75-WA/HT-23 (1975).

3. C. W. Solbrig and E. D. Hughes, *Governing Equations for a Seriated Continuum: An Unequal Velocity Model For Two-Phase Flow,* ANCR-1193 (May 1975).

4. F. H. Harlow and A. A. Amsden, "A Numerical Fluid Dynamics Calculation Method for All Flow Speeds, " *Journal of Computational Physics 8, No. 2* (October 1971) pp 197-213.

5. A. A. Amsden and F. H. Harlow, *KACHINA: An Eulerian Computer Program for Multifield Fluid Flows,* LA-5680 (December 1974).

6. N. Zuber, and F. W. Staub, "The Propagation and the Wave Form of the Vapor Volumetric Concentration in Boiling, Forced Convection System Under Oscillatory Conditions," *International Journal of Heat and Mass Transfer, 9* (1966) pp 871-895.

7. A. V. Kalinin, "Derivation of Fluid Mechanics Equations for a Two-Phase Medium with Phase Changes," *Heat Transfer-Soviet Reserach, 2, No. 3* (1970) pp 83-96.

8. C. W. Solbrig et al, "Heat Transfer and Friction Correlations Required to Describe Steam-Water Behavior in Nuclear Safety Studies," *AIChE Paper No. 21, Presented at the 15th National Heat Transfer Conference, San Francisco, August 10-13, 1975.* Available on microfiche from Oak Ridge National Laboratory as CONF-75084 3, 1976.

9. A. R. Edwards and T. P. O'Brien, "Studies of Phenomena Connected With the Depressurization of Water Reactors," *Journal of the British Nuclear Energy Society, 9* (April 1970) pp 125-135.

10. S. Levy, "Prediction of Two-Phase Critical Flow Rate," *Journal of Heat Transfer, 87* (1965) p 53.

11. W. C. Rivard and M. D. Torrey, *Numerical Calculation of Flashing from Long Pipes Using a Two-Field Model,* LA-6104-M (1975).

DISTRIBUTION RECORD FOR ANCR-NUREG-1340

Internal Distribution

1 - Chicago Patent Group - ERDA
9800 South Cass Avenue
Argonne, Illinois 60439

2-4 - A. T. Morphew
Classification and Technical Information Officer
ERDA - ID
Idaho Falls, Idaho 83401

5 - R. J. Beers, ID

6 - P. E. Litteneker, ID

7 - R. E. Tiller, ID

8 - R. E. Wood, ID

9 - H. P. Pearson, Supervisor
Technical Information

10-19 - INEL Technical Library

20-49 - Authors

50-61 - Special Internal

External Distribution

62-63 - Saul Levine, Director
Office of Nuclear Regulatory Research, NRC
Washington, D. C. 20555

64-374 - Distribution under NRC-4

Total Copies Printed - 374